High-Affinity Partial Agonist Imidazo[1,5-*a*]quinoxaline Amides, Carbamates, and Ureas at the γ-Aminobutyric Acid A/Benzodiazepine Receptor Complex†

E. Jon Jacobsen,*,‡ Ruth E. TenBrink,‡ Lindsay S. Stelzer,‡ Kenneth L. Belonga,‡ Donald B. Carter,§ Haesook K. Im,§ Wha Bin Im,§ Vimala H. Sethy,§ Andy H. Tang,§ Philip F. VonVoigtlander,§ and James D. Petke||

Departments of Medicinal Chemistry, Central Nervous System Diseases Research, and Computational Chemistry, Upjohn Laboratories, The Upjohn Company, Kalamazoo, Michigan 49001

Received November 14, 1994⊗

A series of imidazo[1,5-*a*]quinoxaline amides, carbamates, and ureas which have high affinity for the γ-aminobutyric acid A/benzodiazepine receptor complex was developed. Compounds within this class have varying efficacies ranging from antagonists to full agonists. However, most analogs were found to be partial agonists as indicated by [^{35}S]TBPS and Cl^- current ratios. Many of these compounds were also effective in antagonizing metrazole-induced seizures in accordance with anticonvulsant and possible anxiolytic activity. Selected quinoxalines displayed limited benzodiazepine-type side effects such as ethanol potentiation and physical dependence in animal models. Dimethylamino urea **41** emerged as the most interesting analog, having a partial agonist profile *in vitro* while possessing useful activity in animal models of anxiety such as the Vogel and Geller assays. In accordance with its partial agonist profile, **41** was devoid of typical benzodiazepine side effects.

GABA (γ-aminobutyric acid) is the major inhibitory neurotransmitter in the brain, controlling the excitability of many central nervous system (CNS) pathways. The principal mode of action for this neurotransmitter occurs by modulation of the $GABA_A$ chloride ion channel complex.[1] Numerous chemical classes such as the benzodiazepines, neurosteroids, and barbiturates have binding sites on this macromolecular complex and allosterically modulate the action of GABA on neuronal chloride flux. Of these, compounds which mediate their actions at the benzodiazepine receptor (BzR) are the most widely studied. Ligands which interact at the benzodiazepine (BZD) site have a continuum of intrinsic activity,[2] ranging from full agonists (anxiolytic, hypnotic, and anticonvulsant agents) through antagonists to inverse agonists (proconvulsant and anxiogenic agents). The possibility of partial agonists existing within this continuum is intriguing, as they may be devoid of typical benzodiazepine-mediated side effects such as physical dependence, amnesia, oversedation (anxiolytics), and muscle relaxation or, in the case of inverse agonists, convulsive activity.[3] Furthermore, recent molecular biology studies have demonstrated that several different receptor subunits (α, β, γ, δ) combine to form the $GABA_A$ receptor complex,[4] with at least three to four native receptor subtypes identified thus far.[5] Subtype selective ligands may also allow for the discrimination between useful anxiolytic or hypnotic activity and overt side effects.

Several compounds that are reported to be partial agonists at the benzodiazepine receptor[6−11] are shown in Chart 1. Most of these compounds, abecarnil,[6] bretazenil,[7] alpidem,[9] panadiplon[10] (U-78875), and DN-2327,[11] have undergone clinical trials for the treatment of anxiety disorders. Preliminary results indicate that benzodiazepine-type side effects are lessened for some of these agents, which is consistent with the animal pharmacology. As part of a general structure−activity relationship (SAR) study of U-78875, which was removed from clinical trials due to liver enzyme induction, a new class of imidazo[1,5-*a*]quinoxalines was discovered.[12,13] Leads from this series, as exemplified by structures **1** and **2** (Figure 1), have high affinity for the benzodiazepine receptor complex. More importantly, compounds from this class had varying efficacy, spanning a range from antagonists to full agonists, with several compounds displaying *in vitro* properties consistent with that of a partial agonist.

In order to expand the scope of this series, we were especially interested in modification of the substituent at the 5-position. As reported previously,[12,13] relatively large amide and carbamate substituents could be incorporated into the 5-position of **2**. Most interesting was the possibility of incorporating other substituents at this position to both modify the electronic density and rotational direction of the carbonyl group as well as to further explore the steric requirements of this site. Additional exploration of this series where the 5-substituent was varied to also include ureas and thiocarbamates, and where the A-ring was modified to include 6- and 7-chloro groups was carried out. The 5′-oxadiazole substituent was also varied to include other alkyl groups. Many compounds within this expanded series were partial agonists as determined by *in vitro* analysis. Furthermore, selected urea analogs had good activity in various animal models of anxiety yet displayed limited benzodiazepine-type side effects. Herein we would like to describe the synthesis, *in vitro* efficacy, and pharmacology of this unique class of imidazo[1,5-*a*]quinoxalines. Efforts directed toward the further exploration of the tetracyclic ring system (**1**), where the electronic density and orientation of the carbonyl group is varied systematically, will be reported on shortly.

† A portion of this material was presented at the 207th American Chemical Society National Meeting, March 13−17, 1994.
‡ Department of Medicinal Chemistry.
§ Department of Central Nervous System Diseases Research.
|| Department of Computational Chemistry.
⊗ Abstract published in *Advance ACS Abstracts,* November 15, 1995.

0022-2623/96/1839-0158$12.00/0

Chart 1

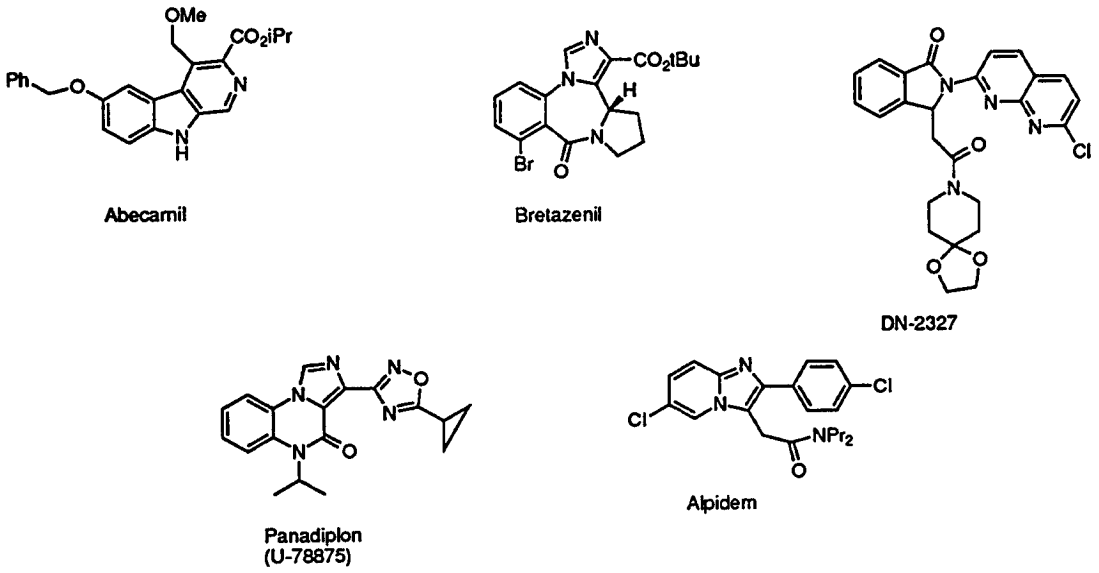

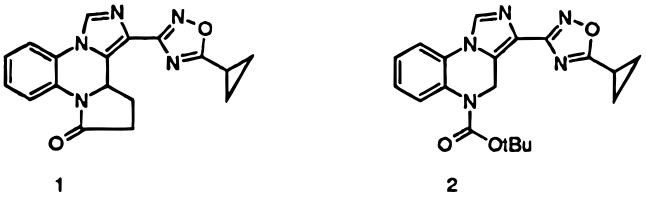

Figure 1.

Chemistry

The general synthesis of the imidazo[1,5-*a*]quinoxalines **7**, **8**, and **10** is shown in Scheme 1. Two methods are applicable, depending on the particular substitution patterns. Reaction of the desired quinoxaline template[12] **3** with potassium *tert*-butoxide, followed by diethyl chlorophosphate, provided an intermediate enol phosphonate, **4**. Without isolation, enol **4** was combined with the desired isocyanide[14] **5** and additional potassium *tert*-butoxide to provide the imidazo[1,5-*a*]quinoxaline **6** ring system. Amides of **6** were formed under standard conditions to provide **7**, whereas selected ureas **8** were formed by reaction of **6** with the desired isocyanate (neat) or carbamoyl chloride. A more general synthesis of urea, carbamate, and thiocarbamate analogs was also developed. Reaction of amine **6** with phosgene or triphosgene in the presence of Hunig's base provided carbamoyl chloride **9**, which was sufficiently stable for long-term storage. However, **9** was most conveniently generated and reacted with the desired nucleophile (amines, alcohols, thiols) *in situ* to provide the appropriate analogs **10**.

An alternative route to *gem*-4-dimethyl analogs of the imidazo[1,5-*a*]quinoxalines, which was found to be particularly useful (but not required), is shown in Scheme 2. In this sequence amine **3** was functionalized at the 5-position with the imidazole ring-forming reaction carried out subsequently. Thus, the carbamoyl chloride of **3** was formed by reaction with phosgene to provide **11**, which could then be reacted directly with the desired nucleophile to give **12**. The imidazole annulation sequence was then carried out as described above to provide the target compound **10**. Table 1 highlights the physical data of the imidazo[1,5-*a*]-quinoxalines prepared by these general methods. Physical data for **33**, **35**, **48**, **66**, and **71** were reported previously.[12]

Several of the requisite quinoxaline starting materials (**3a**−**c**,**g**) were synthesized as previously reported.[12] The corresponding 5- and 6-chloro analogs were prepared as shown in Scheme 3. Following the procedure of Lumma,[15] imine **14** was prepared by reaction of **13** with glyoxylic acid and subsequently reduced with sodium borohydride to provide the 6-chloro isomer **15**. The 5-chloroquinoxaline could not be prepared by this sequence due to poor regioselectivity in the imine cyclization step. Instead, addition of *tert*-butylamine to 2,3-dichloronitrobenzene (**16**) provided nitro **17**, which was reduced with Raney nickel to provide diamine **18**. Acylation of **18** with chloroacetyl chloride and subsequent cyclization provided quinoxaline **19**. Deprotection by treatment of **19** with 2 N sulfuric acid provided a mixture of imine **20** and amine **21** (1:23). The crude mixture was treated with sodium borohydride to give the 5-chloroquinoxaline template (**21**).

The *gem*-3,3-dimethyl-6-chloro template was synthesized as shown in Scheme 4. While 2-amino-2-methylpropionic acid would not add to 2,4-dichloronitrobenzene (**22**), 2-amino-2-methyl-1-propanol (neat, 110 °C) underwent the aromatic nucleophilic substitution in excellent yield to give **23**. Jones oxidation following the procedure of Djerassi[16] provided acid **24**, which was esterified (MeI, K_2CO_3) to give ester **25**. Reduction and *in situ* cyclization of **25** proceeded well, either by reaction with titanium trichloride or by catalytic hydrogenation using sulfur-poisoned Pt/C, to give the quinoxaline template **26**.

A similar cyclization strategy was used for the synthesis of the 5-methyl template **29** as shown in Scheme 5. Alkylation of 2-methyl-6-nitroaniline (**27**) with ethyl bromoacetate provided nitro ester **28**. Reduction of the nitro group and *in situ* cyclization as described above under catalytic hydrogenation conditions resulted in **29**.

The oxadiazole isocyanide reagents were synthesized following the general procedure of Watjen[14] as illustrated in Scheme 6. Acylation of amide oxime **30** with the desired acid halide and cyclization of the

Scheme 1[a]

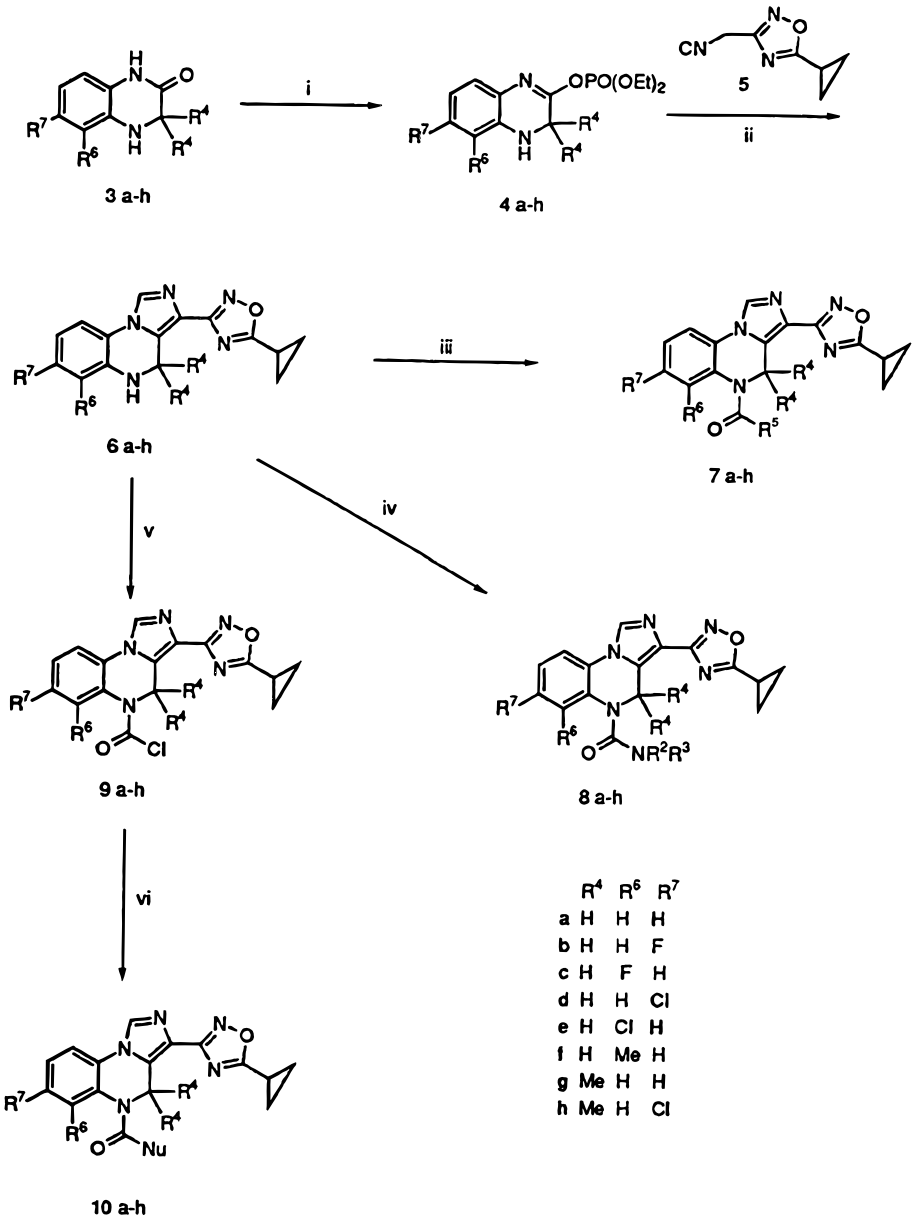

[a]Reagents: (i) (1) 1 N tBuOK, THF, (2) diethyl chlorophosphate; (ii) 1 N tBuOK, THF; (iii) R^5COCl or $(R^5CO)_2O$, THF or CH_2Cl_2, $EtNiPr_2$; (iv) R^2NCO or R^2R^3NCOCl, CH_2Cl_2, $EtNiPr_2$; (v) phosgene in toluene or triphosgene, CH_2Cl_2 or THF, $EtNiPr_2$; (vi) HNu, $EtNiPr_2$.

intermediate by heating in water at reflux provided oxadiazole **31** in good yield. Dehydration of the formamide using phosphorus oxychloride gave the required isocyanide reagents.

Results and Discussion

The binding affinity of the imidazo[1,5-*a*]quinoxalines at the benzodiazepine receptor in rat cortical membranes was determined by competition experiments with radiolabeled [^{3}H]flunitrazepam.[17] The *in vitro* efficacy of these compounds was measured by two different methods. The TBPS ratio[18] was determined for each compound by measuring its effect on *tert*-butyl bicyclophosphorothionate (TBPS) binding to the picrotoxin convulsant site on the $GABA_A$ chloride complex. Changes in TBPS binding presumably occur due to conformational changes in the chloride ionophore caused by allosteric modulation effected by the binding of the test compound to the benzodiazepine receptor. The resultant value, expressed as a ratio of that for the test drug to that of diazepam, is 1 for a full agonist, 0 for an antagonist, and negative values for inverse agonists. A second and more direct measure of *in vitro* efficacy was determined by a $^{36}Cl^-$ uptake assay.[18−20] The synaptic chloride conductance effected by GABA activating the $GABA_A$ receptor complex is modulated by ligands acting at the benzodiazepine receptor. Full agonists increase current, and antagonists have no effect, while inverse agonists decrease ion flow. The test compounds are compared to diazepam, and thus like the TBPS assay, a full agonist has a value of 1 or greater, antagonists having no effect (0), while inverse agonists have negative values. To provide a quick measure of *in vivo* efficacy, most analogs were evaluated for their ability to antagonize metrazole-induced seizures (clonic and tonic).[21] While a direct measure of anticonvulsant activity, this assay is also predictive of anxiolytic properties, as standard full agonist benzodiazepine agents such as diazepam, alprazolam, and zolpidem are extremely effective in this assay, as are partial agonists

Scheme 2[a]

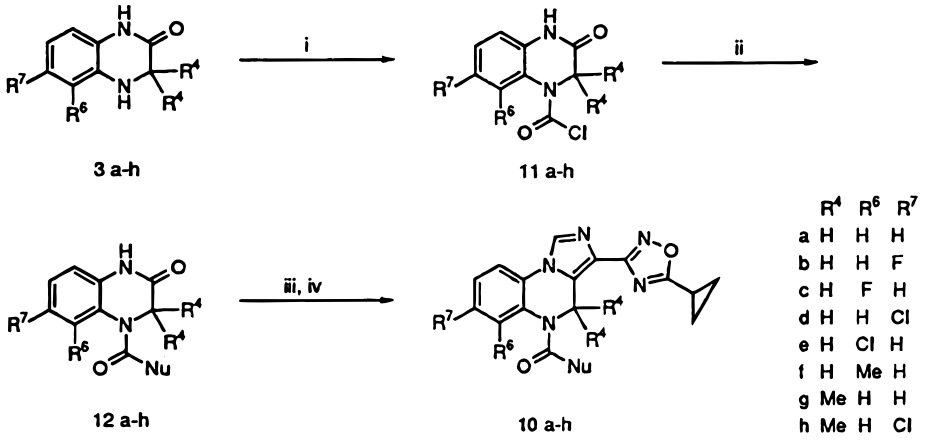

[a]Reagents: (i) phosgene in toluene, CH_2Cl_2 or THF, $EtNiPr_2$; (ii) HNu, $EtNiPr_2$; (iii) 1 N tBuOK, THF, diethyl chlorophosphate; (iv) **5**, 1 N tBuOK, THF.

Table 1. Physical Data for Imidazo[1,5-*a*]quinoxaline Amides, Carbamates, Ureas, and Thiocarbamates

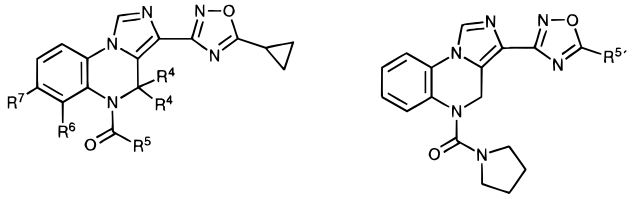

compd	R^4	R^5	R^6	R^7	mp (°C)	method	yield (%)	formula	anal.
34	H	CF_3	H	H	175−177	C	71	$C_{17}H_{12}N_5O_2F_3$	C, H, N, F
36	H	2-pyridine	H	H	239−240	A	30	$C_{21}H_{16}N_6O_2 \cdot {}^1/_4H_2O$	C, H, N
37	H	2-furan	H	H	190−191	I, J	70, 47	$C_{20}H_{15}N_5O_3 \cdot {}^1/_4H_2O$	C, H, N
38	H	2-pyrrole	H	H	252−253	A	64	$C_{20}H_{16}N_6O_2$	C, H, N
39	H	NH_2	H	H	114−115	F	88	$C_{16}H_{14}N_6O_2$	C, H, N
40	H	NHMe	H	H	214−215	D	83	$C_{17}H_{16}N_6O_2 \cdot {}^1/_8H_2O$	C, H, N
41	H	NMe_2	H	H	196−197	B	49	$C_{18}H_{18}N_6O_2 \cdot {}^1/_4H_2O$	C, H, N
42	H	NHEt	H	H	189−190	F	75	$C_{18}H_{18}N_6O_2$	C, H, N
43	H	NEt_2	H	H	173−174	B	37	$C_{20}H_{22}N_6O_2 \cdot {}^1/_4H_2O$	C, H, N
44	H	NHiPr	H	H	210−211	D	58	$C_{19}H_{20}N_6O_2 \cdot H_2O$	C, H, N[a]
45	H	pyrrolidine	H	H	181.5−182.5	F	92	$C_{20}H_{20}N_6O_2$	C, H, N
46	H	morpholine	H	H	198−198.5	F	85	$C_{20}H_{20}N_6O_3 \cdot {}^1/_3H_2O$	C, H, N
47	H	aniline	H	H	211−212.5	D	67	$C_{22}H_{18}N_6O_2$	C, H, N
49	H	OMe	H	H	187−188	E	65	$C_{17}H_{15}N_5O_3$	C, H, N
50	H	OiPr	H	H	207−208	E	58	$C_{19}H_{19}N_5O_3$	C, H, N
51	H	SMe	H	H	176−177	G	95	$C_{17}H_{15}N_5O_2S$	C, H, N, S
52	H	SEt	H	H	169−170	G	69	$C_{18}H_{17}N_5O_2S \cdot {}^1/_4H_2O$	C, H, N, S[b]
53	H	SPh	H	H	222.5−223.5	G	86	$C_{22}H_{17}N_5O_2S \cdot {}^1/_2H_2O$	C, H, N, S[c]
54	H	NMe_2	F	H	194−195	F	88	$C_{18}H_{17}N_6O_2F$	C, H, N
55	H	NMe_2	H	F	227−228.5	F	81	$C_{18}H_{17}N_6O_2F \cdot {}^1/_4H_2O$	C, H, N
56	H	NMe_2	Cl	H	226−228	F	63	$C_{18}H_{17}N_6O_2Cl$	C, H, N, Cl
57	H	NMe_2	H	Cl	254.5−255.5	H, J	80, 55	$C_{18}H_{17}N_6O_2Cl \cdot {}^1/_{20}CH_2Cl_2$	C, H, N, Cl
58	H	pyrrolidine	F	H	220.5−221.5	F	92	$C_{20}H_{19}N_6O_2F$	C, H, N
59	H	pyrrolidine	H	F	203−204	F	82	$C_{20}H_{19}N_6O_2F$	C, H, N
60	H	pyrrolidine	Cl	H	243−244.5	F	75	$C_{20}H_{19}N_6O_2Cl$	C, H, N, Cl
61	H	pyrrolidine	H	Cl	202−204	H, J	82, 54	$C_{20}H_{19}N_6O_2Cl$	C, H, N, Cl
62	H	morpholine	F	H	198.5−201	F	87	$C_{20}H_{19}N_6O_3F$	C, H, N
63	H	morpholine	H	F	224−225	F	75	$C_{20}H_{19}N_6O_3F \cdot {}^1/_3H_2O$	C, H, N
64	H	morpholine	H	Cl	209−210	H, J	57, 59	$C_{20}H_{19}N_6O_3Cl \cdot {}^1/_8H_2O$	C, H, N, Cl
65	H	morpholine	Me	H	265−265.5	F	91	$C_{21}H_{22}N_6O_3 \cdot {}^1/_8H_2O$	C, H, N
67	Me	NH_2	H	H	168−169	F	81	$C_{18}H_{18}N_6O_2 \cdot {}^3/_8H_2O$	C, H, N
68	Me	NHMe	H	H	126−127	F	92	$C_{19}H_{20}N_6O_2$	C, H, N
69	Me	NMe_2	H	H	160−161	F	75	$C_{20}H_{22}N_6O_2$	C, H, N
70	Me	pyrrolidine	H	H	200.5−201.5	F	75	$C_{22}H_{24}N_6O_2$	C, H, N
72	Me	SMe	H	H	163−164	G	93	$C_{19}H_{19}N_5O_2S \cdot {}^1/_8H_2O$	C, H, N, S[d]
73	Me	NMe_2	H	Cl	162−165	H, J	71, 70	$C_{20}H_{21}N_6O_2Cl$	C, H, N, Cl
74	Me	pyrrolidine	H	Cl	207−208	H, J	71, 70	$C_{22}H_{23}N_6O_2Cl$	C, H, N, Cl
75	H	pyrrolidine ($R^{5'}$ = Et)	H	H	190.5−191	H, J	73, 68	$C_{19}H_{20}N_6O_2$	C, H, N
76	H	pyrrolidine ($R^{5'}$ = iPr)	H	H	195−196	H, J	73, 44	$C_{20}H_{22}N_6O_2$	C, H, N
77	H	pyrrolidine ($R^{5'}$ = tBu)	H	H	226−227.5	H, J	73, 62	$C_{21}H_{24}N_6O_2$	C,H,N

[a] N: calcd, 21.98; found, 21.50. [b] S: calcd, 8.62; found, 8.02. [c] S: calcd, 7.55; found, 7.09. [d] S: calcd, 8.36; found, 7.87.

U-78875, bretazenil, and abecarnil,[22] although to a lesser degree.

The effects of substituents at the 5-position in the simple unsubstituted ring system were examined ini-

Scheme 3[a]

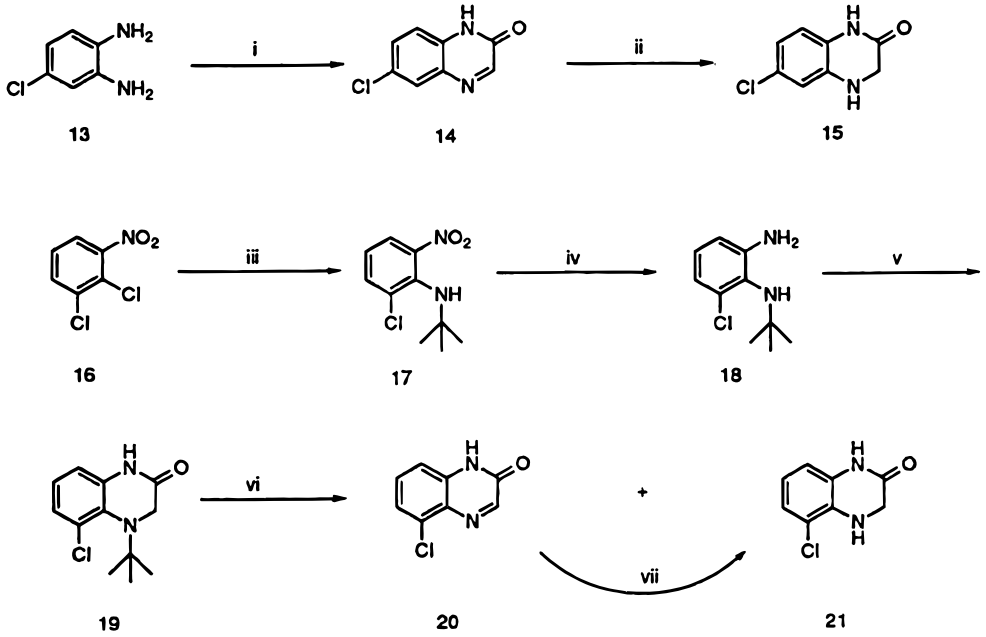

[a]Reagents: (i) glyoxylic acid, MeOH; (ii) $NaBH_4$, EtOH; (iii) $tBuNH_2$, EtOH; (iv) hydrazine hydrate, Raney Ni, EtOH; (v) (1) $ClCH_2CO_2Cl$, $EtNiPr_2$, THF, (2) $EtNiPr_2$, CH_3CN, NaI; (vi) 2 N H_2SO_4; (vii) $NaBH_4$, EtOH.

Scheme 4[a]

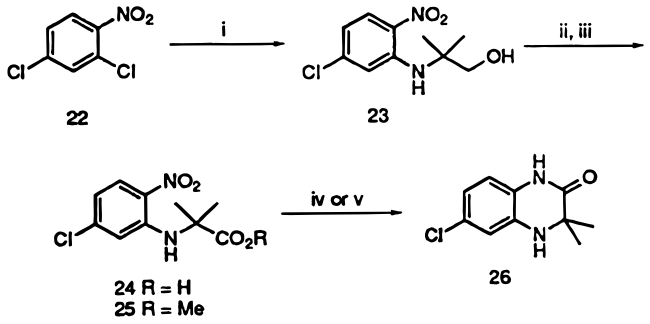

[a]Reagents: (i) 2-amino-2-methyl-1-propanol, 110 °C; (ii) H_2CrO_4, acetone; (iii) MeI, K_2CO_3, DMF; (iv) $TiCl_3$, H_2O, NaOAc, MeOH; (v) sulfided Pt on carbon, EtOH.

Scheme 5[a]

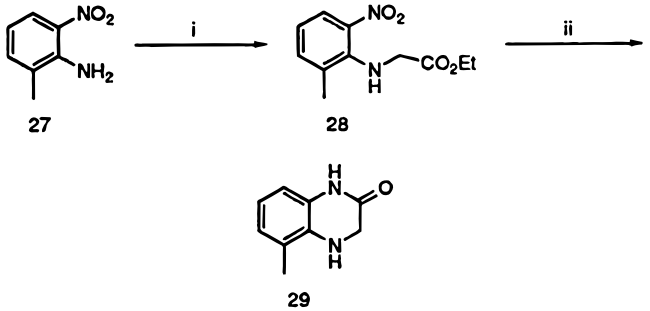

[a]Reagents: (i) $BrCH_2CO_2Et$, $EtNiPr_2$, 140 °C; (ii) H_2, Pd/C, EtOH.

tially. As noted in Table 2, the amides, carbamates, ureas, and thiocarbamates had relatively high affinity for the benzodiazepine receptor on the $GABA_A$ complex, ranging from 0.43 to 16 nM and comparing favorably to standards such as diazepam and zolpidem. The only exception proved to be the electronegative trifluoromethyl acetamide **34**. Other substituents at this position varied substantially in electron-donating character and size yet resulted in only minor changes in affinity. Only the aniline and thiophenol analogs had a significant loss of affinity, whereas less extended but bulky groups (tBu, phenyl, morpholine) were well tolerated. While changes in the 5-substituent had negligible effects on affinity, dramatic differences in efficacy between compounds were noted. By TBPS measurement, most of the amide derivatives were full agonists, particularly those with an electron-rich heterocycle (**37**, **38**). However, the simple benzamide **35** was a partial agonist, while the 2-pyridyl analog **36** was an inverse agonist. The chloride current value for **38** was consistent with this compound being a full agonist, as was its activity in the metrazole antagonism assay. The remaining amide derivatives were substantially less effective as metrazole antagonists, in contrast to what their *in vitro* activity would predict. As a class the urea derivatives were more consistent in this assay. The *in vitro* efficacy for these compounds varied from partial agonists to full agonists based on both the TBPS and chloride current assays. By TBPS measurement, several compounds were full agonists, with **47** having the greatest efficacy. All of the urea analogs were partial agonists in the chloride current screen. No general trends between efficacy and size or the degree of *N*-alkyl substitution were obvious. In the metrazole assay, the cyclic ureas were the most potent anticonvulsant agents followed by the monoalkyl urea analogs, with the disubstituted compounds least effective. Within the urea subseries, several analogs (**39**, **41**, **42**, **45**, **46**) stood out as having excellent metrazole activity combined with partial agonist properties *in vitro*. Analogs in the carbamate and thiocarbamate classes tended to be full agonists as indicated by both the TBPS and chloride current assays. The *tert*-butyl carbamate analog **48** by the TBPS assay had 3-fold greater efficacy than diazepam, further emphasizing the high degree of agonism for this subseries. The metrazole antagonism screen was consistent with the *in vitro* activity, as **48** was extremely effective (0.06 mg/kg). The other carbamate and thiocarbamate analogs were also quite active as metrazole antagonists. Interestingly, thiophenol analog **53**, like the aniline

Scheme 6[a]

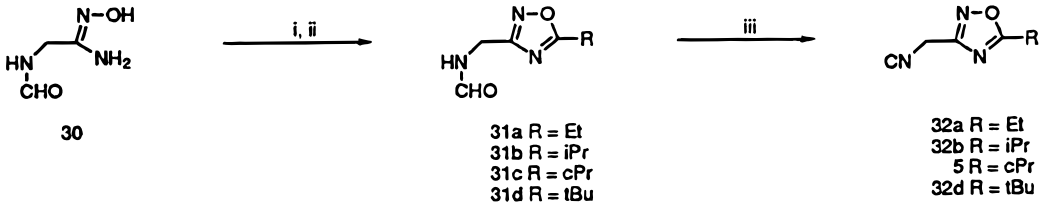

30

31a R = Et
31b R = iPr
31c R = cPr
31d R = tBu

32a R = Et
32b R = iPr
5 R = cPr
32d R = tBu

[a] Reagents: (i) RCOCl, CH_2Cl_2, Et_3N; (ii) H_2O, Δ; (iii) $POCl_3$, Et_3N, CH_2Cl_2.

Table 2. [^{3}H]Fnz Binding, TBPS Shift, $^{36}Cl^-$ Uptake, and Metrazole Antagonism Data for Imidazo[1,5-*a*]quinoxaline Amides, Carbamates, Ureas, and Thiocarbamates

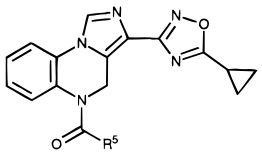

compd	R^5	K_i (nM)[a]	[^{35}S]TBPS shift[b,c]	$^{36}Cl^-$ uptake[b,c]	metrazole[d] ED_{50} (mg/kg, ip)
33	Me	1.5	0.94		35
34	CF_3	143	0.73		35
35	Ph	4.3	0.54		42
36	2-pyridyl	1.1	−0.27		>50
37	2-furan	0.43	0.98	0.55	21
38	2-pyrrole	1.1	0.92	1.1	4.4
39	NH_2	7.2	0.61	0.75	13
40	NHMe	2.8	0.95	0.53	11
41	NMe_2	1.0	0.69	0.68	21
42	NHEt	3.5	0.72	0.22	5.3
43	NEt_2	0.85	0.82	0.62	15
44	NHiPr	3.4	1.1		11
45	pyrrolidine	0.45	0.41	0.50	0.24
46	morpholine	0.81	0.84	0.15	0.84
47	aniline	16	1.3	0.29	>50
48	OtBu	1.9	2.9		0.06
49	OMe	1.5	0.7		4.4
50	OiPr	1.8	1.1		1.9
51	SMe	1.3	0.92	0.73	6.2
52	SEt	2.1	1.1	1.1	1.3
53	SPh	11	1.1	0.50	>50
diazepam		4.9	1.0 ± 0.2	1.0 ± 0.15	0.50 (0.38−1.2)
U-78875		1.6	0.06	0.04	1.6

[a] Mean binding affinity against [^{3}H]flunitrazepam; see ref 17 and the Experimental Section for methods. The standard error was <±10% of the mean. [b] Diazepam is defined as a full agonist which gives a value of 1. Antagonists are defined as having a shift value of 0; partial agonists are intermediate. [c] See the Experimental Section. [d] Antagonism of metrazole-induced clonic convulsions in the rat after ip injection; see the Experimental Section.

analog in the urea series, was completely inactive in the metrazole screen, indicating possible rapid metabolism or poor CNS bioavailability for these aryl analogs.

As selected urea analogs had a desirable partial agonist profile combined with good activity in the primary *in vivo* screen, further modifications at other positions on this template usually maintained the 5-substituent as either a dimethylamino, pyrrolidino, or morpholino urea. As shown in Table 3, the incorporation of either a fluoro or chloro group at the 6- or 7-position had little effect on affinity. Only the 7-chloro analogs show a slight decrease in binding affinity within each urea subseries. With the dimethylamino and pyrrolidino urea analogs, halogenation generally increased efficacy by TBPS measurement, except for the 6-chloro derivatives, which had similar values to the unsubstituted parents. The 7-fluoro and 7-chloro derivatives generally had higher chloride current ratios than the 6-halo or unsubstituted analogs. In the metrazole antagonism screen, most of the halogenated analogs in this subseries were much less effective than the parent compounds, even though their *in vitro* efficacy was often greater. The only exceptions were **54** and **61**, which were roughly equivalent to the unsubstituted analogs. As a class, the morpholine ureas were somewhat dissimilar. By TBPS measurement, only the 7-fluoro analog **63** had greater efficacy than the parent. In contrast, the halogenated and 6-methyl analogs all had greater efficacy by chloride current measurement, with **63** and **64** being full agonists. In addition, all the morpholine derivatives tested were active in antagonizing metrazole-induced seizures (although to a lesser degree than unsubstituted **46**), in contrast to the dimethylamino and pyrrolidino analogs. The 6-methyl (**65**) and 6-fluoro (**62**) analogs were particularly impressive having potent metrazole activity, greater than expected considering their *in vitro* partial agonist profile. Nonetheless, within this series, substitution at the 6- or 7-position with chloro, fluoro, or methyl groups, while often providing increased efficacy, usually resulted in diminished activity *in vivo*.

Biological data for compounds incorporating *gem*-dimethyl groups at the 4-position are provided in Table 4. As compared to the unsubstituted analogs, *gem*-

Table 3. [^{3}H]Fnz Binding, TBPS Shift, $^{36}Cl^-$ Uptake, and Metrazole Antagonism Data for Imidazo[1,5-*a*]quinoxaline Ureas with Fluoro, Chloro, or Methyl A-Ring Substituents

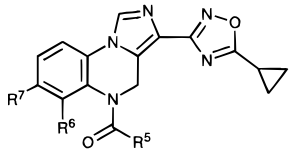

compd	R^5	R^6	R^7	K_i (nM)[a]	[^{35}S]TBPS shift[b,c]	$^{36}Cl^-$ uptake[b,c]	metrazole[d] ED_{50} (mg/kg, ip)
41	NMe_2	H	H	1.0	0.69	0.68	21
54	NMe_2	F	H	0.89	0.84	0.60	21
55	NMe_2	H	F	0.61	0.99	0.95	
56	NMe_2	Cl	H	0.71	0.62	0.83	>50
57	NMe_2	H	Cl	3.7	0.88		
45	pyrrolidine	H	H	0.45	0.41		0.24
58	pyrrolidine	F	H	0.64	1.0	0.59	>50
59	pyrrolidine	H	F	0.56	1.25	0.69	>50
60	pyrrolidine	Cl	H	0.73	0.60	0.56	>50
61	pyrrolidine	H	Cl	1.1	0.93		0.60
46	morpholine	H	H	0.81	0.84	0.15	0.84
62	morpholine	F	H	0.48	0.66	0.42	6.2
63	morpholine	H	F	0.68	0.96	1.1	6.2
64	morpholine	H	Cl	2.3	0.71	1.0	
65	morpholine	Me	H	4.6	0.51	0.70	5.2

[a] Mean binding affinity against [^{3}H]flunitrazepam; see ref 17 and the Experimental Section for methods. The standard error was <±10% of the mean. [b] Diazepam is defined as a full agonist which gives a value of 1. Antagonists are defined as having a shift value of 0; partial agonists are intermediate. [c] See the Experimental Section. [d] Antagonism of metrazole-induced clonic convulsions in the rat after ip injection; see the Experimental Section.

Table 4. [^{3}H]Fnz Binding, TBPS Shift, $^{36}Cl^-$ Uptake, and Metrazole Antagonism Data for Imidazo[1,5-*a*]quinoxaline Amides, Carbamates, Ureas, and Thiocarbamates with *gem*-4,4-Dimethyl Substitution

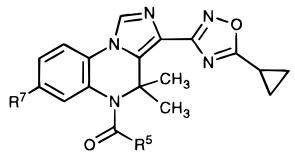

compd	R^5	R^7	K_i (nM)[a]	[^{35}S]TBPS shift[b,c]	^{36}Cl uptake[b,c]	metrazole[d] ED_{50} (mg/kg, ip)
66	Me	H	4.9	0.70		30
67	NH_2	H	86	0.60	0.22	>50
68	NHMe	H	21	0.71	0.67	>50
69	NMe_2	H	3.1	0.97	0.34	>50
70	pyrrolidine	H	2.9	0.84	0.50	>50
71	OMe	H	6.8	0.8	0.4	>50
72	SMe	H	5.1	0.80	1.0	>50
73	NMe_2	Cl	3.1	0.79	1.33	7.4
74	pyrrolidine	Cl	3.3	0.67	1.04	35

[a] Mean binding affinity against [^{3}H]flunitrazepam; see ref 17 and the Experimental Section for methods. The standard error was <±10% of the mean. [b] Diazepam is defined as a full agonist which gives a value of 1. Antagonists are defined as having a shift value of 0; partial agonists are intermediate. [c] See the Experimental Section. [d] Antagonism of metrazole-induced clonic convulsions in the rat after ip injection; see the Experimental Section.

dimethyl substitution lowered affinity substantially, between 3- and 12-fold. The only exception proved to be **73**, which had a K_i of 3.1 nM, roughly comparable to that of **57**. In contrast, the primary urea analog **67** suffered the greatest loss of affinity with increased substitution. The effects of the *gem*-dimethyl groups on efficacy were mixed. By TBPS shift measurement, both **69** and **70** had significantly increased efficacy, while most of the other analogs displayed little change over the unsubstituted parent compounds. Interestingly, the methylurea analog **68** had significantly lower efficacy as compared to **40**. A lack of a definitive trend was also noted for these analogs in the chloride current assay. However, even though *gem*-dimethyl substitution usually maintained or increased efficacy by *in vitro* analysis, almost all of the compounds were inactive in the metrazole screen. The only effective compound was **73**, with an ED_{50} of 7.4 mg/kg, while **74** and **66** were marginally active, although **74** was 50-fold less potent than the unsubstituted analog. For the most part, substitution with methyl groups at the 4-position had a minimal effect on *in vitro* activity while having a deleterious effect on *in vivo* activity. This diminished activity for the 4,4-dimethyl analogs in the metrazole and other *in vivo* assays may relate to increased metabolism for this substitution pattern.

The 3′-substituent on the oxadiazole was also varied, with data for several representative structures provided in Table 5. Reasonable binding affinity was maintained across the series except for the *tert*-butyl analog, which had 15-fold decreased affinity as compared to the other analogs. A general trend in the *in vitro* properties for both the TBPS and chloride current assays was noted, as compounds containing bulkier substituents had

Table 5. [^{3}H]Fnz Binding, TBPS Shift, $^{36}Cl^-$ Uptake, and Metrazole Antagonism Data for Imidazo[1,5-*a*]quinoxaline Ureas with Selected 5′-Alkyloxadiazole Substituents

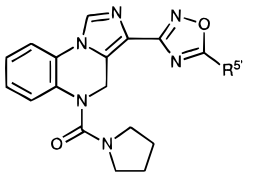

compd	R$^{5'}$	K_i (nM)[a]	[^{35}S]TBPS shift[b,c]	$^{36}Cl^-$ uptake[b,c]	metrazole[d] ED_{50} (mg/kg, ip)
75	Et	0.65	0.39	0.25	>50
76	iPr	1.1	0.69	0.40	11
45	cPr	0.45	0.41	0.50	0.24
77	tBu	14.7	0.76	1.2	18

[a] Mean binding affinity against [^{3}H]flunitrazepam; see ref 17 and the Experimental Section for methods. The standard error was <±10% of the mean. [b] Diazepam is defined as a full agonist which gives a value of 1. Antagonists are defined as having a shift value of 0; partial agonists are intermediate. [c] See the Experimental Section. [d] Antagonism of metrazole-induced clonic convulsions in the rat after ip injection; see the Experimental Section.

enhanced efficacy. This correlation of efficacy to steric bulk was particularly evident in the chloride current assay where the 5′-ethyl analog was nearly an antagonist, while the *tert*-butyl derivative was a full agonist. On the other hand, activity in the metrazole assay did not parallel the *in vitro* results. Instead the cyclopropyl analog was superior to the other more efficacious analogs. While the diminished activity of **77** in this assay is explainable by affinity differences, the lack of potent anticonvulsant activity for the other oxadiazole analogs is less clear.

The frequent lack of correlation between the TBPS shift ratio, Cl^- current, and *in vivo* activity for compounds within this series, and benzodiazepine ligands in general, can be partially attributed to heterogeneity of the GABA$_A$ receptor population. Classical benzodiazepines interact with the $\alpha_1\beta_2\gamma_2$, $\alpha_2\beta_2\gamma_2$, $\alpha_3\beta_2\gamma_2$, and $\alpha_5\beta_2\gamma_2$ subtypes with nearly equal affinity,[23] while atypical BzR ligands such as Cl 218 872 and Zolpidem have moderate selectivity for the $\alpha_1\beta_2\gamma_2$ subtype.[4a,23] However, classical benzodiazepines do not interact with the $\alpha_6\beta_2\gamma_2$ subtype located in cerebellar granule cells, whereas ligands such as Ro 15-4513 have high affinity for this subtype.[24] Furthermore, these BzR ligands often display efficacy selectivity, where Cl^- current is modulated to varying degrees in these receptor subtypes.[25] The search for selective ligands for these subtypes as well as the elucidation of their function remains an important goal in this area.

A few analogs from this series were examined in several different benzodiazepine receptor subtypes.[26,27] As reported previously,[12,13] these quinoxalines have excellent affinity for the $\alpha_1\beta_2\gamma_2$ subtype with binding data for a selected number of compounds shown in Table 6. The affinity of all analogs evaluated in the $\alpha_3\beta_2\gamma_2$ subtype was also quite high, although usually 2−9-fold less than for $\alpha_1\beta_2\gamma_2$. Most analogs within this series were not evaluated in these binding assays given the general lack of selectivity observed between these two subtypes. Affinity of selected analogs for the $\alpha_6\beta_2\gamma_2$ subtype was extremely poor with only the small 5-acetamide substituent of **33** tolerated.[12,13] Even then, at least a 45-fold drop in affinity between the $\alpha_1\beta_2\gamma_2$ and $\alpha_6\beta_2\gamma_2$ subtypes was noted.

Table 6. [^{3}H]Fnz Binding in $\alpha_1\beta_2\gamma_2$, $\alpha_3\beta_2\gamma_2$, and $\alpha_6\beta_2\gamma_2$ Subtypes and $^{36}Cl^-$ Uptake in $\alpha_1\beta_2\gamma_2$ and $\alpha_3\beta_2\gamma_2$ Subtypes for Imidazo[1,5-*a*]quinoxaline Ureas and Amides

	K_i (nM)[a]			Cl^- uptake[c,d]	
compd	$\alpha_1\beta_2\gamma_2$	$\alpha_3\beta_2\gamma_2$	$\alpha_6\beta_2\gamma_2$[b]	$\alpha_1\beta_2\gamma_2$	$\alpha_3\beta_2\gamma_2$
33	2.7		124		
35	0.3		1140		
39				0.75	0.52
41	1.7	3.5		0.68	0.74
42	4.5	15			
46				0.15	0.55
55				0.95	0.83
58				0.59	0.36
62	0.17	0.51	13%		
63	0.30	0.70		1.1	0.60
64	0.22	2.0	0%		
65	4.7	30	0%		
67				0.22	0.0
68				0.67	0.78
73				1.3	0.62
diazepam	13	10	>7000	1.0 ± 0.15	1.0 ± 0.15
Ro 15-4513	15 ± 4		5.4 ± 0.4		
U-78875	3.5	5.7	603		

[a] The ability of the compounds to displace [^{3}H]flunitrazepam was measured in membranes from Sf-9 insect cells expressing the $\alpha_1\beta_2\gamma_2$ and $\alpha_3\beta_2\gamma_2$ subtypes and to displace [^{3}H]Ro 15-4513 in insect cell membranes expressing the $\alpha_6\beta_2\gamma_2$ subtype, as described in the Experimental Section. [b] Percent inhibition at 100 nM. [c] Diazepam is defined as a full agonist which gives a value of 1. Antagonists are defined as having a shift value of 0; partial agonists are intermediate. [d] See the Experimental Section.

While all analogs were evaluated for efficacy using the Cl^- current assay in the $\alpha_1\beta_2\gamma_2$ subtype, several derivatives were screened in the $\alpha_3\beta_2\gamma_2$ subtype. Three analogs (**46**, **63**, **73**) had significantly different efficacy between the two subtypes. Interestingly with morpholine **46**, efficacy was enhanced in the $\alpha_3\beta_2\gamma_2$ subtype, whereas **63** and **73** displayed full agonist efficacy in the $\alpha_1\beta_2\gamma_2$ subtype and a partial agonist profile in $\alpha_3\beta_2\gamma_2$. Not surprisingly, **46** and **73** also displayed the greatest differences between the TBPS (evaluated in the native GABA$_A$ receptor population) and Cl^- current ($\alpha_1\beta_2\gamma_2$) values. Several analogs were also identified which had a partial agonist profile in both subtypes. Of particular interest were partial agonists **39**, **41**, and **46** ($\alpha_1\beta_2\gamma_2$ and $\alpha_3\beta_2\gamma_2$ subtypes), which also displayed potent activity in the metrazole assay. Analogs within this series were not evaluated for efficacy in the $\alpha_6\beta_2\gamma_2$ subtype due to low affinity.

While only a limited study was carried out for compounds within this series in these receptor subtypes, the binding differences between the $\alpha_6\beta_2\gamma_2$ and other subtypes are consistent with a sterically restricted region in the $\alpha_6\beta_2\gamma_2$ subtype that cannot accommodate the rather large (out-of-plane) 5-substituent of these analogs.[13] In addition, like the benzodiazepines and related compounds, little binding or efficacy selectivity between the $\alpha_1\beta_2\gamma_2$ and $\alpha_3\beta_2\gamma_2$ subtypes was evident for most of the analogs in this series. Nonetheless, significant differences in efficacy for three compounds between these subtypes were noted, providing promise for the future discovery of efficacy selective analogs within the quinoxaline urea class.

On the basis of the results of the *in vitro* (binding, TBPS, chloride current) and metrazole assays, several of the most promising compounds were evaluated further for typical benzodiazepine-type side effects, with data provided in Table 7. Two of the more undesirable side effects typically promoted by benzodiazepine full

Table 7. Benzodiazepine Antagonism, Ethanol Potentiation, and Acute Physical Dependence Data for Imidazo[1,5-*a*]quinoxaline Ureas

compd	BZD antag traction[a] ED_{50} (mg/kg)	ethanol potentiation ED_{50} (mg/kg) traction[a]	ethanol potentiation ED_{50} (mg/kg) LRR	acute electroshock physical dependence activity[a] (drug MA_{50}/V122 MA_{50})
40	22	2.7	11	A (18.9/21.5)
41	1	27	>30	IA (23.2/24.9)
42	>30	>30	>30	IA (19.7/20.4)
43	4	>30	>30	IA (20.9/21.5)
51	>30	0.3	>30	A (17.7/22.4)
54	4	3	>30	A (17.7/20.3)
61	>30	0.4	>30	IA (21.0/22.4)
62				A (14.4/21.2)
63	1	2	>30	A (20.7/24.1)
73		3	17	A (17.2/19.3)
74	9	0.2	>30	IA (19.4/19.3)
76	>30	17	>30	IA (22.1/22.1)
diazepam		0.54 (0.54−0.54)	0.86 (0.5−1.4)	A[b] (18.2/25.4)
U-78875	1.7 (0.8−3.8)	6.6 (3.3−13)	>30	IA (21.2/22.2)

[a] See the Experimental Section. [b] Tested at 15 mg/kg.

agonists are ethanol potentiation and physical dependence. The potentiation of the effects of alcohol by the test compounds was determined by measuring the drug ED_{50}s for traction and the loss of righting after coadministration. In this assay, diazepam was quite potent, having ED_{50} values of 0.54 and 0.86 mg/kg for traction and loss of righting, respectively. The degree of acute physical dependence was assessed through an electroshock seizure assay.[28] Withdrawal from chronic treatment with high doses of benzodiazepines may in some cases result in signs and symptoms related to hyperexcitability of the CNS. In animals, such changes can be quantified by determining the current threshold (MA_{50}) to elicit electroshock-induced seizures. In this assay, the lowering of electroshock thresholds precipitated by a benzodiazepine antagonist after an acute regimen of test compound was used to quantify the development of physical dependence. Mice received the test drug for 3 days (150 mg/kg/day). Twenty-four hours after the last administration, the mice received an iv injection of a benzodiazepine antagonist (flumazenil). Five minutes later, the mice were assessed for electroshock seizure thresholds (MA_{50} compared to vehicle MA_{50}), which typically were lower for mice undergoing flumazenil-precipitated withdrawal. Standard benzodiazepine ligands such as diazepam were active in this paradigm at doses as low as 15 mg/kg/day. Finally, most of the compounds were evaluated for their ability to antagonize the muscle relaxation effects of a benzodiazepine full agonist, triazolam. Traction was assessed 30 min after separate administration of triazolam and the test compound. The antagonist flumazenil, at 2.0 mg/kg, was effective in blocking the muscle-relaxing effects of triazolam, as was the partial agonist U-78875 (1.7 mg/kg). Traditional full agonist benzodiazepine ligands are not effective in blocking muscle relaxation in this assay.

Most of the quinoxaline analogs that were evaluated in the ethanol potentiation assay had little effect on the loss of righting reflex, consistent with their partial agonist profile. Only **40** and **73** were active, although to a much lesser degree than diazepam. However, like U-78875, many of the quinoxalines did have effects on traction, although usually to a lesser degree than diazepam. Compounds **41**−**43** in particular stand out as being relatively free of ethanol interaction. Roughly one-half of the compounds tested were active in the physical dependence assay. Even though these compounds were tested at 10 times the dose of diazepam, any significant activity in this assay was considered undesirable. The two analogs that significantly altered the loss of righting reflex were also found to be active in the physical dependence screen and, not unexpectedly, were full agonists in the *in vitro* efficacy assays. However, for other compounds, the correlation of the TBPS and chloride current assays to activity in the physical dependence screen was quite poor, perhaps due to differences in pharmacokinetics or varying receptor subtype interactions. Many of the quinoxalines tested were active to some degree in antagonizing the effects of triazolam. The most potent compounds were **41**, **43**, **54**, and **63**. Nonetheless, only two of these analogs were inactive in the acute electroshock dependence assay, indicating that even a moderately potent benzodiazepine antagonist can still produce undesirable side effects.

On the basis of its overall profile in these screens, **41** was selected for detailed evaluation in several other assays useful for predicting anxiolytic activity. In Vogel's punished licking assay[10a] (Figure 2), this quinoxaline was effective in increasing the number of shocks taken at doses ranging between 0.3 and 10 mg/kg. The activity of **41** in this assay was equieffective to that of 1.0 mg/kg diazepam (DZ). Similarly, in the Geller−Cook conflict assay,[10a] **41** was active in punished animals at doses of 0.3, 1.0, and 3.0 mg/kg (Figure 3). Significant activity was also nearly achieved at lower doses. No effects were observed in the nonpunished **41** group. Again the activity of this compound compared quite favorably to that achieved by diazepam (data not shown). The morpholine analog **63** was also active in both of these assays as shown in Figures 2 and 3.

Molecular Conformations. The low-energy conformers of a representative set of compounds were determined by molecular mechanics methods. Calculations were performed using both the AMBER* and MM2* force fields, which were developed for the MacroModel[29] system of programs as extensions of the original AMBER[30] and MM2[31] parameter sets. Initial structures to be minimized were generated by means of an internal coordinate Monte Carlo procedure[32] in which torsional angles around all rotatable bonds were allowed to vary. The analogs examined by these methods are listed in Table 8.

In Figure 4, structures of the two lowest-energy conformers of **41** obtained with the MM2* force field are shown. The structures are identical except for the

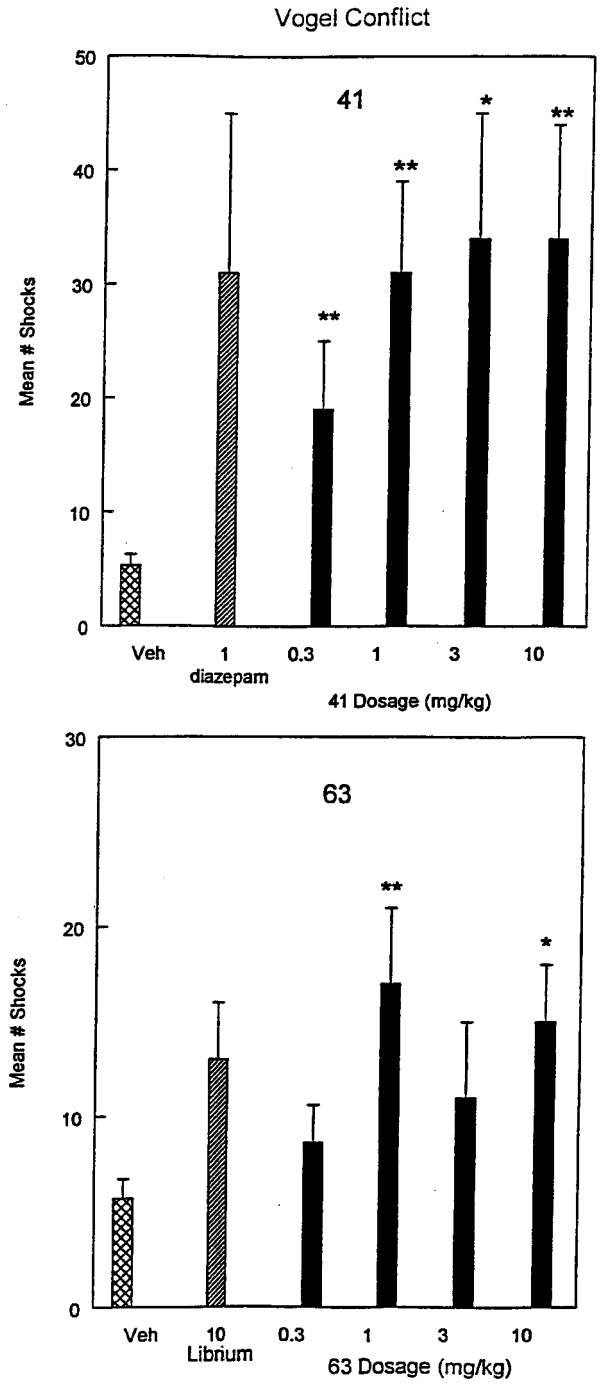

Figure 2. Vogel conflict assay. Bar graphs of the mean number of shocks received after drinking for each dose group. Compound **41** or **63** was injected ip 30 min prior to the test session with 8−10 animals/group. Statistical comparison between vehicle- and drug-treated animals was carried out by one-way analysis of variance followed by the nonparametric Wilcoxon rank sum test for each treatment group (* = p < 0.05; ** = p < 0.01).

orientations of the R^5 substituent, which differ by a 180° rotation about the N_5−C bond. Calculations using the AMBER* force field yielded structures with no significant geometrical differences from those obtained with MM2*, both for **41** and all other analogs for which calculations were performed. It should be noted that for each structure shown, there exists a pair of conformational enantiomers of identical energy, which differ geometrically due to the puckering of the imidazoquinoxaline ring.

Figure 5 shows structure A for three urea analogs (**39**, **41**, **45**) in an edge view of the imidazoquinoxaline ring. For each analog shown, as well as all others unsubstituted at the 4-position, the ring system is nearly planar, with the oxadiazole ring rotated out of the imidazole plane by only 5°. For the 4,4-*gem*-dimethyl-substituted analogs **67**, **69**, and **70**, the preferred orientation of the oxadiazole ring is ca. 30° out of the imidazole plane due to electrostatic interactions between $N_{4'}$ and the methyl groups. The R^5 substituent is seen to occupy an out-of-plane region, similar to that of the C_5-phenyl group in classical benzodiazepines. The position of the R^5 group is not significantly altered by 4,4-*gem*-dimethyl substitution.

While the molecular structures obtained from the respective force fields were found to be very similar, the same does not apply to relative energies. Specifically, the data in Table 8 show that structure A is the lowest-energy conformer according to MM2*, but AMBER* favors structure B as that of lowest energy except for the *gem*-dimethyl-substituted analogs **67**, **69**, and **70**. Thus, in general, the preferred conformation cannot be determined unequivocally from the present studies. In many cases, the computed energy difference between structures A and B is not large, and a mixture of conformations may exist. However, as discussed further below, the N_5−C rotation barrier is such that conversion between the two conformers may not readily occur. In this regard, the orientation of the carbonyl group appears to be unimportant as a factor in receptor binding, since it can be physically constrained to point in relatively different orientations as in **1** and isomers cyclized from N_5−C_6 via lactam rings[33] as illustrated for **78** (Figure 6). Analogs from both of these constrained ring systems have excellent affinity for the BzR.

In order to obtain an indication of the flexibility of the present analogs, estimates of selected rotation barriers were obtained from a series of constrained molecular mechanics energy minimizations. The following gives ranges of values obtained from studies on the analogs in Table 8 using both AMBER* and MM2* parameters. The cyclopropyl group is free to rotate about the $C_{5'}$−C bond with a barrier of only 1.4−1.7 kcal/mol. Rotation of the oxadiazole group about C_3−$C_{3'}$ is subject to a moderate barrier of 5−7 kcal/mol. The methyl groups in the *gem*-dimethyl-substituted analogs do not change the rotation barrier significantly. As may be expected, rotation about N_5−C bond appeared to be severely restricted, and barrier heights could not be obtained in most cases. Calculations performed on the N_5-formyl analog, in which changes in formyl orientation were accompanied by significant distortions of the quinoxaline ring, yielded an estimate of 12−17 kcal/mol.

Pharmacophore Models. A number of models have been proposed in order to elucidate the steric and electronic properties necessary for BzR recognition and activation.[34] For the present analogs, both structures A and B of Figure 4 exhibit several features consistent with general models proposed by Wermuth et al.[35] and Gardner.[36] As depicted in Figure 7, the fused phenyl component of the quinoxaline ring and the N_2 atom act as the aromatic region and hydrogen acceptor site (δ_1), respectively, regarded as the principal features necessary for receptor recognition.[34−37] The cyclopropyl oxa-

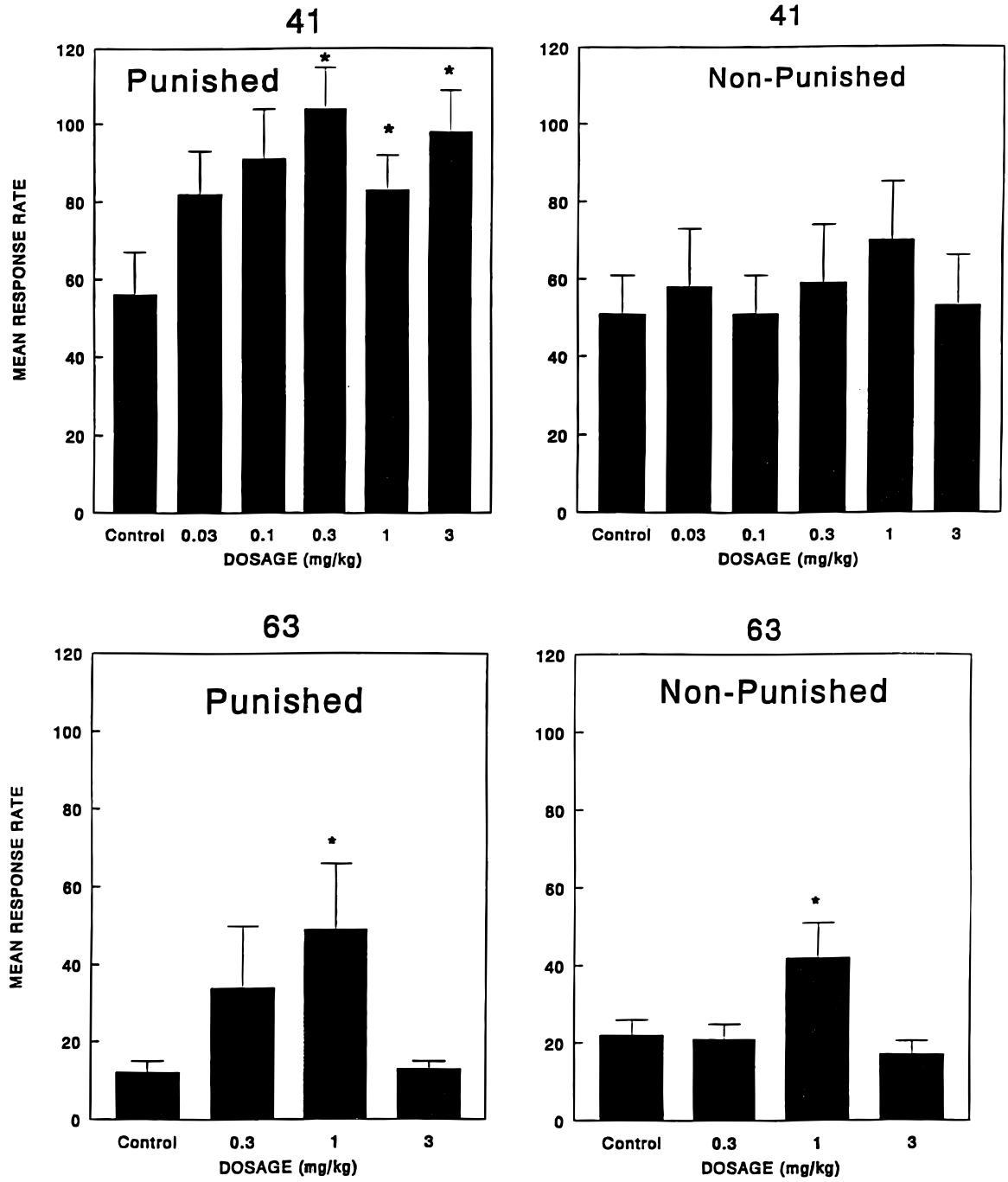

Figure 3. Geller–Cook conflict assay. Bar graphs of the mean response rate of lever pressing for food reinforcement. Animals were trained to press a lever to receive a food pellet for a 5 min period followed by a 2 min punished period where food was accompanied by an electric shock, signaled by a light over the response lever. Compounds **41** and **63** were injected ip 30 min before the test session with 6 animals/dose group. Wilcoxon signed-rank tests were used to compare data from each dosing group with their own control data (* = $p < 0.05$).

diazole group in the present analogs correlates with both the "freely-rotating aromatic" group in the Wermuth model, and the ester group cited in the Gardner model. This feature is absent in classical benzodiazepines but is present in a number of forms including aromatic, ester, acyl, or oxadiazole groups in other BzR ligands. According to both models, efficacy may be modulated by altering either the lipophilic character and/or the physical size of this substructure, which is supported in the present study by the limited data given in Table 5. Perhaps most significantly, the R^5 substituent which distinguishes this series from most other BzR ligands, corresponds to the "out-of-plane" region described by Wermuth. This site is thought to correlate with full agonist activity,[34,35] which may explain how the 5-substituent in the present analogs can successfully modulate efficacy. The only other major class of BzR ligands that have a nonaromatic substituent at this site is the cyclopyrrolones,[35,36] with the piperazine side chain of Zopiclone located in the same region as the R^5 substituent (e.g., **45**) when an overlay of the δ_1 and aromatic regions is performed. Interestingly, the electronegative carbonyl group of the R^5 substituent probably does not correspond to the δ_2 hydrogen acceptor site in the Wermuth model (see Figure 7) as it is located out of the aryl plane and has a significantly greater distance to the imidazole hydrogen acceptor site (δ_1) than typically observed: 6.0–6.5 Å, depending on the conformational

Table 8. Relative Energies of Low-Energy Conformers of Selected Imidazo[1,5-*a*]quinoxaline Amides, Ureas, and Carbamates

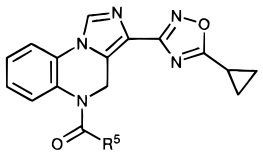

		relative energies (kcal/mol)			
		AMBER*		MM2*	
compd	R^5	A	B	A	B
33	Me	1.29	0.00	0.00	2.08
35	phenyl	1.00	0.00	0.00	1.79
39	NH_2	0.00	0.24	0.00	2.61
41	NMe_2	1.03	0.00	0.00	2.52
45	pyrrolidine	1.12	0.00	0.00	2.13
48	OtBu	2.94	0.00	0.00	1.67
49	OMe	3.04	0.00	0.00	1.96
50	OiPr	2.96	0.00	0.00	1.63
67[a]	NH_2	0.00	1.72	0.00	3.82
69[a]	NMe_2	0.00	3.42	0.00	6.79
70[a]	pyrrolidine	0.00	3.54	0.00	7.00

[a] 4,4-*gem*-Dimethyl substituted.

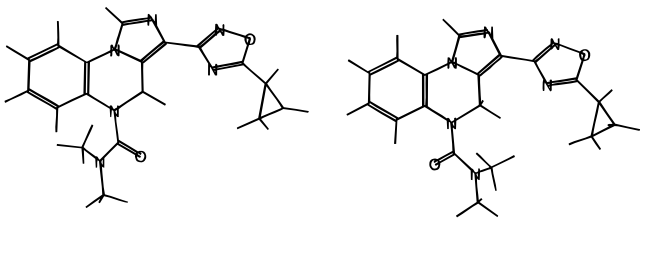

A B

Figure 4. Molecular structures of the two lowest-energy conformers of **41**.

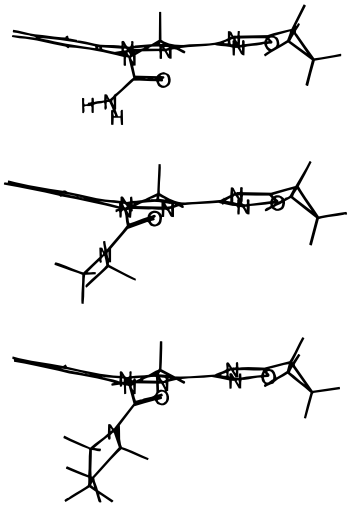

Figure 5. Edge view of molecular structures of conformer A for **39**, **41**, and **45**.

isomer vs 3.2 Å for standard BZDs. Given the similar affinity of compounds from this series to **1** and **78**, it is arguable that if the carbonyl group is acting as the δ_2 hydrogen acceptor, then this site in this series plays a greater role in modulating efficacy than affinity. In summary, the present analogs are consistent with a model in which an aromatic region and single hydrogen acceptor site act as necessary components for receptor recognition, while efficacy is governed by the cooperative

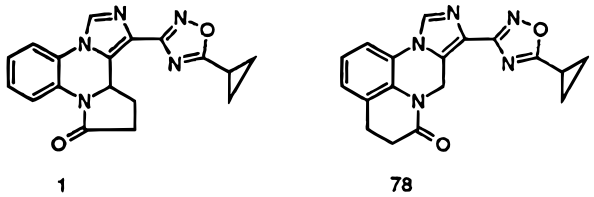

1 **78**

Figure 6.

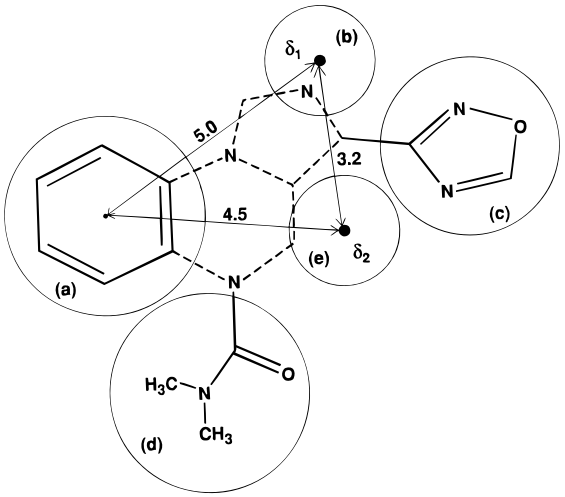

Figure 7. Structure of **41** showing elements of the Wermuth and Gardner pharmacophore models: (a) aromatic region, (b) hydrogen acceptor site δ_1, (c) freely-rotating unit, and (d) out-of-plane region. The second hydrogen acceptor site (δ_2, e) is absent in the present analogs. Distances shown between a, b, and e are given in angstroms.

effects of the R^3 substituent coplanar with the quinoxaline ring and the out-of-plane R^5 substituent.

Conclusion

Compounds within this imidazo[1,5-*a*]quinoxaline series are high-affinity ligands for the GABA$_A$/benzodiazepine receptor. By control of the substituents at the 4-, 5-, 6-, and 7-positions, analogs spanning a wide range of efficacy, from antagonists to full agonists, were prepared. Most importantly, particularly for the 5-urea quinoxalines, compounds with a partial agonist profile were identified. Many of these compounds were active in selected animal models of anxiety or sedation. Furthermore, in line with the partial agonist hypothesis, side effects such as physical dependence, ethanol potentiation, and muscle relaxation were significantly reduced as compared to benzodiazepine full agonists. From this series, **41** stands out as having minimal benzodiazepine side effects yet is equieffective to diazepam in classical animal models of anxiety such as the Vogel and Geller paradigms. The continued evaluation of **41** and the further exploration of this series in the search of GABA$_A$-derived anxiolytic partial agonists will be reported in due course.

Experimental Section

Chemistry. Thin-layer and flash chromatography utilized E. Merck silica gel (230−400 mesh). Melting points were taken on a Thomas-Hoover capillary melting point apparatus and are uncorrected. Mass spectra, infrared spectra, and combustion analysis were obtained by the Physical and Analytical Chemistry Department of The Upjohn Co. ^{1}H NMR spectra were recorded at 300 MHz with a Bruker Model AM-300 spectrometer.

In cases where synthetic intermediates or products were isolated by "aqueous workup (organic solvent, drying agent)", the procedure was to quench the reaction with H_2O, dilute with the indicated organic solvent, separate the organic layer, extract the aqueous layer several times with the organic solvent, dry the combined organic layers with the indicated drying agent, filter off the drying agent, and remove solvent using a rotary evaporator at reduced pressure. When "basic workup (organic solvent, aqueous basic solvent, drying agent)" is indicated, the procedure was similar to aqueous workup, except the indicated aqueous base was used instead of H_2O. When "acidic workup (organic solvent, organic solvent, drying agent)" is indicated, the procedure was to dilute the reaction mixture with the first indicated solvent, extract the organic solution several times with 10% HCl, basify the combined acidic layers with solid KOH, extract the basic solution with the second indicated organic solvent several times, dry the organic layers with the indicated drying agent, filter off the drying agent, and remove solvent using a rotary evaporator under reduced pressure. Tetrahydrofuran (THF) and ether were distilled from sodium and benzophenone. Dichloromethane was distilled from calcium hydride, and DMF was dried over 3 Å molecular sieves. All other solvents were EM Science HPLC grade, distilled in glass. Diethyl chlorophosphate and potassium *tert*-butoxide (1.0 M in THF) were purchased from the Aldrich Chemical Co., Milwaukee, WI. Phosgene in toluene (**CAUTION**: phosgene is highly toxic and should be used with extreme care) was purchased from Fluka Chemie AG or Columbia. All reactions were run under nitrogen or argon.

Preparation of Amide Templates 3. 1,2,3,4-Tetrahydroquinoxalin-2-one (**3a**), 3,3-dimethyl-1,2,3,4-tetrahydroquinoxalin-2-one (**3g**), 5-fluoro-1,2,3,4-tetrahydroquinoxalin-2-one (**3c**), and 6-fluoro-1,2,3,4-tetrahydroquinoxalin-2-one (**3b**) were prepared as previously described.[12]

6-Chloro-1,2-dihydroquinoxalin-2-one (14). Following the procedure of Lumma,[15] glyoxylic acid (29.4 mL, 266 mmol, 50% aqueous) was added to a solution of 4-chloro-1,2-phenylenediamine (**13**; 38.0 g, 266 mmol) and MeOH (1.87 L) at 15 °C. The dark black solution was stirred for 24 h at room temperature and concentrated. The residue was washed with water (4 × 608 mL) and 2-propanol (145 mL) and dried *in vacuo* to give 45.1 g of a black solid. Two successive recrystallizations from hot (ca. 90 °C) 2-methoxyethanol (1.49 and 0.927 L) gave 18.0 g (37%) of **14** as a gray powder: ^{1}H NMR (300 MHz, DMSO-d_6) δ 12.55 (br s, NH), 8.22 (s, N=CH), 7.86 (narrow m, ArH), 7.62 (dd, J = 8.4, 1.5 Hz, ArH), 7.32 (d, J = 8.7 Hz, ArH).

6-Chloro-1,2,3,4-tetrahydroquinoxalin-2-one (15). Sodium borohydride (5.10 g, 135 mmol) was added to a mixture of imine **14** (5.60 g, 31.0 mmol) and ethanol (200 mL). The resultant solution was stirred for 2.5 h at room temperature and concentrated. Aqueous workup (ethyl acetate, $MgSO_4$) and recrystallization from ethyl acetate−hexane gave (two lots) 4.19 g of amine **15**. The filtrate was concentrated and purified by flash chromatography (1:1 hexane:ethyl acetate) to provide 451 mg (after recrystallization) of additional product (4.64 g total, 82%) as a light brown powder (mp 171−174 °C): IR (mineral oil) 1687, 1517, 1408, 1307, 1299 cm^{-1}; ^{1}H NMR (300 MHz, $CDCl_3$−MeOD) δ 6.6−6.75 (m, ArH), 3.95 (s, NCH_2CO); MS (EI) m/e 182, 153.

***N*-*tert*-Butyl-6-chloro-2-nitroaniline (17).** A mixture of 2,3-dichloronitrobenzene (**16**; 92.5 g, 482 mmol), *tert*-butylamine (138 mL, 1.31 mol), and 50 mL of ethanol was heated in a bomb at 150 °C for 3 days. After cooling to room temperature, concentration and aqueous workup (CH_2Cl_2, Na_2SO_4) gave 107 g (97%) of **17** as a brown oil: IR (neat) 2970, 1532, 1484, 1447, 1366, 1348, 1192, 755 cm^{-1}; ^{1}H NMR (300 MHz, $CDCl_3$) δ 7.73 (dd, J = 8.2, 1.6 Hz, ArH), 7.61 (dd, J = 8.0, 1.6 Hz, ArH), 7.07 (apparent t, J = 8.1 Hz, ArH), 4.77 (s, NH), 1.22 (s, $C(CH_3)_3$); MS (EI) m/e 172, 154, 142, 126, 114, 99, 90.

2-(*tert*-Butylamino)-3-chloroaniline (18). A solution of hydrazine monohydrate (115 mL, 2.37 mol) in 270 mL of ethanol was added dropwise with stirring over 30 min to a 0 °C mixture of **17** (108 g, 472 mmol), Raney nickel (27 g, finely divided, Aldrich 22,167−8, slurry in water at pH 10), and 540 mL of ethanol. The mixture was stirred for 90 min at 0 °C. Filtration and aqueous workup (Et_2O, Na_2SO_4) gave 91.7 g (98%) of **18** as a brown oil which was used without further purification: ^{1}H NMR (300 MHz, $CDCl_3$) δ 6.82 (apparent t, J = 7.8 Hz, ArH), 6.75 (dd, J = 7.9, 1.6 Hz, ArH), 6.60 (dd, J = 7.7, 1.7 Hz, ArH), 4.11 (br s, NH_2), 3.02 (br s, NH), 1.26 (s, $C(CH_3)_3$).

4-*tert*-Butyl-5-chloro-1,2,3,4-tetrahydroquinoxalin-2-one (19). Chloroacetyl chloride (55.2 mL, 693 mmol) was added dropwise with stirring over 1 h to a −78 °C solution of diamine **18** (91.7 g, 462 mmol) and diisopropylethylamine (241 mL, 1.38 mol) in 900 mL of THF. The mixture was allowed to warm slowly and stirred at room temperature for 18 h. Basic workup (CH_2Cl_2, $NaHCO_3$, Na_2SO_4) of the concentrated mixture gave an uncyclized amide intermediate as a black oil: ^{1}H NMR (300 MHz, $CDCl_3$) δ 9.74 (br s, CONH), 8.33 (d, J = 7.6 Hz, ArH), 7.05−7.2 (m, ArH, 2 H), 4.20 (s, CH_2), 3.07 (s, N**H**C-$(CH_3)_3$), 1.24 (s, $C(CH_3)_3$).

A solution of the intermediate and diisopropylethylamine (120 mL, 689 mmol) in 1.50 L of acetonitrile was heated at reflux in the presence of sodium iodide (9.00 g, 60.0 mmol) for 18 h. Aqueous workup (CH_2Cl_2, Na_2SO_4) of the concentrated mixture gave the crude product as a black, oily solid. Flash chromatography (10% acetone/hexane) and trituration (CH_2Cl_2) gave 12.1 g of **19** as a white solid (mp 197.5−198.5 °C). The filtrate was concentrated, rechromatographed, and triturated (5:30:65, v/v, MeOH:Et_2O:hexane) to give 18.8 g of additional product. Flash chromatography of the filtrate (1% MeOH/CH_2Cl_2) gave an additional 1.22 g of **19**. The total yield of **19** was 32.1 g (29%): IR (mineral oil) 1677, 1579, 1367, 1187, 778 cm^{-1}; ^{1}H NMR (300 MHz, $CDCl_3$) δ 8.05 (br s, NH), 7.0−7.15 (m, ArH, 2 H), 6.73 (d, J = 7.6 Hz, ArH), 3.72 (ABq, J_{AB} = 17.3 Hz, $\Delta\nu$ = 169 Hz, CH_2), 1.27 (s, $C(CH_3)_3$); MS (EI) m/e 238, 223, 182, 153, 90, 57.

5-Chloro-1,2,3,4-tetrahydroquinoxalin-2-one (21). A suspension of *tert*-butyl-protected amide **19** (32.1 g, 134 mmol) in 500 mL of 2 N H_2SO_4 was stirred at room temperature for 18 h. The solids were filtered, washed with aqueous $NaHCO_3$ and water, and dried at room temperature to give 23.6 g (96%) of a 23:1 mixture of **21** and the corresponding imine **20** as determined by ^{1}H NMR integration of the amide hydrogen resonances at δ 12.62 for **20** and δ 10.47 for **21**.

Sodium borohydride (1.84 g, 48.6 mmol) was added in one portion to a 0 °C slurry of the crude amine/imine mixture (20.5 g, 113 mmol) in 680 mL of EtOH. The mixture was allowed to warm to room temperature and stirred for 2 h. The ethanol was evaporated, and the solids were triturated with water, filtered, washed with water, and dried to give 19.5 g (95%) of **21** as a tan solid (mp 191−193 °C): IR (mineral oil) 3407, 1690, 1503, 1426, 771 cm^{-1}; ^{1}H NMR (300 MHz, DMSO-d_6) δ 10.47 (s, CONH), 6.89 (d, J = 8.0 Hz, ArH), 6.70 (d, J = 7.0 Hz, ArH), 6.59 (apparent t, J = 7.9 Hz, ArH), 5.84 (s, CH_2N**H**), 3.80 (d, J = 1.8 Hz, NHC**H**$_2$); MS (EI) m/e 182, 153.

2-[*N*-(5-Chloro-2-nitrophenyl)amino]-2-methyl-1-propanol (23). A solution of 2,4-dichloronitrobenzene (**22**; 20.0 g, 0.104 mol) and 2-amino-2-methyl-1-propanol (80 mL, 0.84 mol) was stirred at 110 °C for 68 h. After cooling to room temperature, aqueous workup (CH_2Cl_2, $MgSO_4$) gave 26.9 g of **23**, sufficiently pure (>90%) to be carried on crude. An analytical sample was prepared by recrystallization from ethyl acetate−hexane to provide orange crystals (mp 102−104 °C): IR (mineral oil) 3335, 1610, 1577, 1492, 1331, 1251, 1154, 748 cm^{-1}; ^{1}H NMR (300 MHz, $CDCl_3$) δ 8.55 (br s, NH), 8.13 (d, J = 9.2 Hz, ArH), 7.09 (d, J = 2.1 Hz, ArH), 6.59 (dd, J = 9.2, 2.0 Hz, ArH), 3.71 (s, C**H**$_2$OH), 2.11 (br s, OH), 1.48 (s, $C(CH_3)_2$); MS (EI) m/e 244, 213, 166.

***N*-(5-Chloro-2-nitrophenyl)-2-methylalanine (24).** Jones reagent[16] (2.67 M) was added in aliquots (40, 20, 20, 20, and 10 mL) every 15 min to a solution of crude alcohol **23** (26.9 g) and acetone (2.05 L) at 0 °C until the reaction was done by TLC analysis. 2-Propanol (150 mL) was added, and the mixture was allowed to warm to room temperature. The mixture was filtered, and the solids washed with acetone several times. The combined filtrates were concentrated and partitioned between ether (800 mL) and 10% potassium

hydroxide (3 × 100 mL). The basic layers were acidified (3 N HCl) and extracted with CH_2Cl_2 (3 × 180 mL). The CH_2Cl_2 layers were dried ($MgSO_4$), filtered, and concentrated to provide 16.2 g (60% from **22**) of carboxylic acid **24** as a yellow powder (mp 146−147 °C): IR (mineral oil) 3363, 1707, 1613, 1573, 1495, 1336, 1272, 1241, 753 cm^{-1}; ^{1}H NMR (300 MHz, $CDCl_3$) δ 8.48 (br s, NH), 8.16 (d, J = 9.1 Hz, ArH), 6.68 (dd, J = 9.1, 2.0 Hz, ArH), 6.64 (d, J = 2.0 Hz, ArH), 1.74 (s, $C(CH_3)_2$); MS (EI) *m*/*e* 258, 213.

***N*-(5-Chloro-2-nitrophenyl)-2-methylalanine Methyl Ester (25).** A mixture of acid **24** (22.3 g, 86.2 mmol), DMF (260 mL), potassium carbonate (35.6 g, 0.258 mol), and iodomethane (26.9 mL, 0.432 mol) was stirred at room temperature for 16 h. Aqueous workup (ether, water and brine washes, $MgSO_4$) gave 22.0 g (94%) of ester **25** as an orange solid (mp 87−89 °C): IR (mineral oil) 3349, 1737, 1606, 1489, 1330, 1263, 1230, 1149, 752 cm^{-1}; ^{1}H NMR (300 MHz, $CDCl_3$) δ 8.48 (br s, NH), 8.15 (d, J = 9.1 Hz, ArH), 6.65 (dd, J = 9.1, 2.1 Hz, ArH), 6.54 (d, J = 2.1 Hz, ArH), 3.77 (s, OCH_3), 1.69 (s, $C(CH_3)_2$); MS (EI) *m*/*e* 272, 213.

6-Chloro-3,3-dimethyl-1,2,3,4-tetrahydroquinoxalin-2-one (26). Aqueous titanium trichloride (20%, 260 mL) was added dropwise over 10 min to a mixture of nitro compound **25** (14.1 g, 51.7 mmol), sodium acetate (240 g, 2.93 mol), MeOH (504 mL), and water (156 mL). The light blue mixture was stirred for 2.5 h at room temperature. Basic workup (ethyl acetate, $NaHCO_3$, brine wash, $MgSO_4$) gave 10.8 g (99%) of amide **26** as a tan powder (mp 166−170 °C) homogeneous by TLC analysis: IR (mineral oil) 3311, 1658, 1614, 1505, 1404, 1355 cm^{-1}; ^{1}H NMR (300 MHz, $CDCl_3$) δ 8.67 (br s, CONH), 6.73 (dd, J = 8.3, 2.0 Hz, ArH), 6.6−6.7 (m, ArH, 2 H), 3.78 (s, NH), 1.42 (s, $C(CH_3)_2$); MS (FAB) *m*/*e* 210, 195, 167.

***N*-(2-Methyl-6-nitrophenyl)glycine Ethyl Ester (28).** A mixture of 2-methyl-6-nitroaniline (**27**; 2.00 g, 13.1 mmol), ethyl bromoacetate (3.5 mL, 32 mmol), and diisopropylethylamine (3.5 mL, 20 mmol) was heated at reflux (140 °C) for 8 h. The resultant solution was allowed to cool to room temperature. After a basic workup ($CHCl_3$, $NaHCO_3$, $MgSO_4$), the residue was resubmitted to the above reaction conditions for an additional 16 h. After workup, purification by flash chromatography (10:1 → 5:1 hexane:ethyl acetate) gave 681 mg (22%) of **28** as a glassy yellow solid (mp 49−52 °C): IR (mineral oil) 3365, 1731, 1536, 1475, 1344, 1236, 1207, 1104, 1022 cm^{-1}; ^{1}H NMR (300 MHz, $CDCl_3$) δ 7.88 (d, J = 8.5 Hz, ArH), 7.33 (d, J = 8.8 Hz, ArH), 6.8−7.0 (m, NH), 6.86 (apparent t, J = 7.8 Hz, ArH), 4.17 (q, J = 7.1 Hz, C**H**$_2$CH$_3$), 3.94 (d, J = 6.0 Hz, NHC**H**$_2$), 2.39 (s, CH_3Ar), 1.23 (t, J = 7.1 Hz, CH_2C**H**$_3$); MS (EI) *m*/*e* 238, 165, 118, 107, 91.

6-Methyl-1,2,3,4-tetrahydroquinoxalin-2-one (29). A mixture of nitro compound **28** (675 mg, 2.83 mmol), ethanol (60.0 mL), and 10% Pd/C (150 mg) was hydrogenated (48 psi) at room temperature for 3.5 h. The mixture was filtered, the residue was washed with ethanol, and the combined filtrates were concentrated to provide 425 mg (93%) of amide **29** as a tan powder (mp 168−171 °C): IR (mineral oil) 3382, 1671, 1490, 1444, 1393, 1295, 770 cm^{-1}; ^{1}H NMR (300 MHz, $CDCl_3$) δ 8.68 (br s, NHCO), 6.79 (d, J = 7.7 Hz, ArH), 6.6−6.75 (m, ArH, 2 H), 4.04 (s, NHC**H**$_2$), 3.76 (br s, N**H**CH$_2$), 2.17 (s, CH_3Ar); MS (EI) *m*/*e* 162, 133.

Example Procedure for Oxadiazole 31: 3-[(*N*-Formylamino)methyl]-5-*tert*-butyl-1,2,4-oxadiazole (31d). A solution of trimethylacetyl chloride (6.82 mL, 55.4 mmol) in methylene chloride (10 mL) was added dropwise over 10 min to a cold suspension of (*N*-formylamino)acetamide oxime triethylamine[14] (**30**; 10.9 g, 49.9 mmol) and triethylamine (11.9 mL, 85.4 mmol) in methylene chloride (80 mL) at 0 °C. The resultant slurry was stirred at 0 °C for 1 h and at room temperature for 22 h. The mixture was concentrated, diluted with 75 mL of water, and heated at reflux for 48 h. After cooling to room temperature, aqueous workup (CH_2Cl_2, $MgSO_4$) and purification by flash chromatography (1:1 ethyl acetate: methylene chloride) gave 6.18 g (68%) of **31d** as a yellow liquid: ^{1}H NMR (300 MHz, $CDCl_3$) δ 8.32 (s, CHO), 6.0−6.3 (m, NH), 4.63 (d, J = 5.6 Hz, NHC**H**$_2$), 1.44 (s, tBu).

Example Procedure for Isocyanide 32: 3-(Isocyanomethyl)-5-*tert*-butyl-1,2,4-oxadiazole (32d). Triethylamine (14.1 mL, 101 mmol) was added to a mixture of formamide **31d** (6.18 g, 33.7 mmol) and methylene chloride (77 mL) at 0 °C. Phosphorus oxychloride (3.14 mL, 33.7 mmol) was added slowly and the solution stirred for 1 h at 0 °C. The reaction was quenched with aqueous sodium carbonate (3.57 g Na_2CO_3 in 39 mL of H_2O), and the mixture was stirred for an additional 15 min at 0 °C before being allowed to warm to room temperature. Aqueous workup (CH_2Cl_2, $MgSO_4$) and purification by flash chromatography (2:1 hexane:ethyl acetate) gave 4.71 g (85%) of **32d** as an amber liquid: ^{1}H NMR (300 MHz, $CDCl_3$) δ 4.73 (s, $CNCH_2$), 1.46 (s, tBu).

Example Procedure for the Synthesis of 3-(5-Cyclopropyl-1,2,4-oxadiazol-3-yl)-4,5-dihydroimidazo[1,5-*a*]quinoxalines 6: 6-Chloro-3-(5-cyclopropyl-1,2,4-oxadiazol-3-yl)-4,5-dihydroimidazo[1,5-*a*]quinoxaline (6e). A solution of amide **3e** (2.63 g, 14.4 mmol) in 30 mL of THF was cooled to −40 °C, and potassium *tert*-butoxide (1.0 M in THF, 15.8 mL, 15.8 mmol) was added dropwise over 5 min. The mixture was allowed to warm to room temperature over 30 min and then cooled to −50 °C. Diethyl chlorophosphate (2.70 mL, 18.7 mmol) was added dropwise over 4 min, and the mixture was allowed to warm from −50 to −30 °C over 1 h and then allowed to warm to room temperature over 30 min. The solution was cooled to −78 °C, and isocyanide **5** (2.58 g, 17.3 mmol) was added. Potassium *tert*-butoxide (17.3 mL, 17.3 mmol) was added dropwise over 10 min. The mixture was allowed to warm slowly to room temperature and stirred at room temperature overnight. The mixture was diluted with water; the solids were filtered, washed, and dried to give 3.26 g (72%) of **6e** as a white solid (mp 205−207 °C): IR (mineral oil) 3327, 1571, 1493, 1305, 773 cm^{-1}; ^{1}H NMR (300 MHz, $CDCl_3$) δ 8.06 (s, ArH), 7.34 (d, J = 8.0 Hz, ArH), 7.19 (d, J = 7.0 Hz, ArH), 6.78 (apparent t, J = 8.1 Hz, ArH), 4.89 (d, J = 1.6 Hz, NHC**H**$_2$), 4.67 (s, NH), 2.2−2.3 (m, C**H**CH$_2$), 1.2−1.4 (m, CH_2CH_2); MS (EI) *m*/*e* 313, 244, 229.

3-(5-Cyclopropyl-1,2,4-oxadiazol-3-yl)-4,4-dimethyl-4,5-dihydroimidazo[1,5-*a*]quinoxaline (**6g**), 3-(5-cyclopropyl-1,2,4-oxadiazol-3-yl)-4,5-dihydroimidazo[1,5-*a*]quinoxaline (**6a**), 3-(5-cyclopropyl-1,2,4-oxadiazol-3-yl)-7-fluoro-4,5-dihydroimidazo[1,5-*a*]quinoxaline (**6b**), and 3-(5-cyclopropyl-1,2,4-oxadiazol-3-yl)-6-fluoro-4,5-dihydroimidazo[1,5-*a*]quinoxaline (**6c**) were synthesized as previously reported.[12]

Example Procedures for the Acylation of Quinoxaline 6. Method A: 3-(5-Cyclopropyl-1,2,4-oxadiazol-3-yl)-4,5-dihydro-5-(2-pyrrolylcarbonyl)imidazo[1,5-*a*]quinoxaline (38). The pyrrole acid chloride was prepared by the procedure of Maxim.[38] A mixture of **6a** (600 mg, 2.15 mmol), the acid halide (389 mg, 3.00 mmol), diisopropylethylamine (1.05 mL, 6.03 mmol), and THF (15.0 mL) was stirred at room temperature for 16 h. Additional acid halide (200 mg, 1.54 mmol) and diisopropylethylamine (0.50 mL, 2.9 mmol) were added, and the mixture was stirred for an additional 5 h, at which time no starting material was evident by TLC analysis. Basic workup (ethyl acetate and then $CHCl_3$, $NaHCO_3$, $MgSO_4$) and two successive recrystallizations from hot ethyl acetate/MeOH gave 365 mg of **38** as white plates (mp 252−253 °C). The filtrate was concentrated and recrystallized as above to provide an additional 144 mg (509 mg total, 64%) of the amide: IR (mineral oil) 3120, 1643, 1579, 1509, 1401, 1359, 1294, 1037, 767 cm^{-1}; ^{1}H NMR (300 MHz, $CDCl_3$) δ 9.49 (br s, NH), 8.15 (s, ArH), 7.59 (apparent t, J = 9.2 Hz, ArH, 2 H), 7.2−7.4 (m, ArH, 2 H), 6.95 (s, ArH), 6.30 (s, ArH), 6.17 (narrow m, ArH), 5.49 (s, CH_2N), 2.2−2.35 (m, C**H**CH$_2$CH$_2$), 1.15−1.4 (m, CHC**H**$_2$C**H**$_2$); MS (EI) *m*/*e* 372, 304, 279, 210, 195, 94. Anal. ($C_{20}H_{16}N_6O_2$) C, H, N.

Method B: 3-(5-Cyclopropyl-1,2,4-oxadiazol-3-yl)-5-[(dimethylamino)carbonyl]-4,5-dihydroimidazo[1,5-*a*]quinoxaline (41). A mixture of dimethylcarbamyl chloride (539 mg, 5.01 mmol), pyridine (10 mL), and imidazoquinoxaline **6a** (700 mg, 2.51 mmol) was stirred for 10 min at room temperature. Basic workup (CH_2Cl_2, $NaHCO_3$, Na_2SO_4) provided a mixture of product and starting material. The residue was combined with dimethylcarbamyl chloride (10.0 mL, 109 mmol) and 30 mL of pyridine, and the mixture was stirred at room temperature for 19 h. Identical workup gave a solid that was absorbed onto 10 g of Celite. Flash chromatography with

15% EtOAc/CH_2Cl_2 followed by 50% EtOAc/CH_2Cl_2 afforded 431 mg (49%) of **41** as an off-white solid (mp 196−197 °C): IR (mineral oil) 1664, 1573, 1500, 1275, 1202, 756 cm^{-1}; ^1H NMR (300 MHz, $CDCl_3$) δ 8.11 (s, ArH), 7.54 (d, J = 6.7 Hz, ArH), 7.2−7.3 (m, ArH), 7.05−7.2 (m, ArH, 2 H), 4.99 (s, NCH_2), 2.85 (s, NMe_2), 2.2−2.3 (m, CH), 1.2−1.4 (m, CH_2CH_2); MS (EI) *m/e*, 350, 306, 278, 263, 238, 210, 195, 72. Anal. ($C_{18}H_{18}N_6O_2 \cdot {}^1/_4H_2O$) C, H, N.

Method C: 3-(5-Cyclopropyl-1,2,4-oxadiazol-3-yl)-4,5-dihydro-5-(trifluoroacetyl)imidazo[1,5-*a*]quinoxaline (34). Trifluoroacetic anhydride (0.28 mL, 2.0 mmol) was added to a mixture of **6a** (500 mg, 1.79 mmol) and pyridine (4.0 mL). The resultant solution was stirred for 16 h at room temperature. Basic workup ($CHCl_3$, $NaHCO_3$, $MgSO_4$) and recrystallization from ethyl acetate−hexane (two crops) gave 477 mg (71%) of the trifluoroacetamide as a light brown powder (mp 175−177 °C): IR (mineral oil) 1707, 1604, 1512, 1498, 1432, 1424, 1419, 1283, 1218, 1211, 1205, 1194, 1163, 1154, 1087, 768 cm^{-1}; ^1H NMR (300 MHz, $CDCl_3$) δ 8.16 (s, ArH), 7.88 (br s, ArH), 7.63 (d, J = 8.4 Hz, ArH), 7.35−7.55 (m, ArH, 2 H), 5.38 (s, NCH_2), 2.2−2.35 (m, C**H**CH_2), 1.2−1.4 (m, CH_2CH_2); MS (EI) *m/e* 375, 306, 278, 210. Anal. ($C_{17}H_{12}N_5O_2F_3$) C, H, N, F.

Example Procedure for the Reaction of 6 with Isocyanates. Method D: 3-(5-Cyclopropyl-1,2,4-oxadiazol-3-yl)-4,5-dihydro-5-[(methylamino)carbonyl]imidazo[1,5-*a*]quinoxaline (40). Imidazoquinoxaline **6a** (600 mg, 2.15 mmol) was stirred with 10 mL of methyl isocyanate at 40 °C for 3 days. The mixture was diluted with hexane and filtered. The solids were triturated with copious amounts of hexane and dried to give 600 mg (83%) of the product as a white solid (mp 214−215 °C): IR (mineral oil) 3374, 3100, 1655, 1575, 1503, 767 cm^{-1}; ^1H NMR (300 MHz, $CDCl_3$) δ 8.10 (s, ArH), 7.5−7.65 (m, ArH, 2 H), 7.2−7.4 (m, ArH, 2 H), 5.26 (s, CH_2), 5.06 (s, NH), 2.75−2.90 (m, NCH_3), 2.2−2.3 (m, CH), 1.15−1.4 (m, CH_2CH_2); MS (EI) *m/e* 336, 279, 238, 210, 195, 69. Anal. ($C_{17}H_{16}N_6O_2 \cdot {}^1/_8H_2O$) C, H, N.

Example Procedure for Carbamoyl Chloride 9: 5-(Chlorocarbonyl)-3-(5-cyclopropyl-1,2,4-oxadiazol-3-yl)-4,5-dihydroimidazo[1,5-*a*]quinoxaline (9a). Phosgene (39.4 mL, 43.0 mmol, 1.09 M in toluene) was added dropwise to a slurry of amine **6a** (4.00 g, 14.3 mmol), THF (80 mL), and diisopropylethylamine (7.5 mL, 43 mmol). The mixture was stirred at room temperature for 19 h. The excess phosgene was decomposed with ice and $NaHCO_3$. Aqueous workup (CH_2Cl_2, Na_2SO_4) and crystallization from CH_2Cl_2/hexane gave 4.15 g (85%) of **9a** as a white solid (mp 164−165 °C): ^1H NMR (300 MHz, $CDCl_3$) δ 8.16 (s, ArH), 7.8−7.95 (m, ArH), 7.6−7.65 (m, ArH), 7.35−7.55 (m, ArH, 2 H), 5.50 (br s, NCH_2), 2.2−2.35 (m, CH), 1.2−1.4 (m, CH_2CH_2).

Example Procedures for the Reaction of Carbamoyl Chloride 9 with Selected Nucleophiles. With Alcohols, Method E: 3-(5-Cyclopropyl-1,2,4-oxadiazol-3-yl)-4,5-dihydro-5-(methoxycarbonyl)imidazo[1,5-*a*]quinoxaline (49). A solution of carbamoyl chloride **9a** (500 mg, 1.46 mmol) and THF (3.0 mL) was added to a solution of sodium methoxide (95 mg, 1.8 mmol) and MeOH (2.0 mL) at 0 °C. The solution was allowed to warm to room temperature and stirred for 2 h. The reaction was quenched with 1 mL of water, and the solution was concentrated. Aqueous workup (EtOAc, $MgSO_4$) and recrystallization of the crude solid from EtOAc/hexane provided 318 mg (65%) of **49** as a yellow powder (mp 187−188 °C): IR (mineral oil) 1714, 1514, 1504, 1444, 1301, 1291, 1221, 1207, 764, 757 cm^{-1}; ^1H NMR (300 MHz, $CDCl_3$) δ 8.11 (s, ArH), 7.78 (d, J = 7.0 Hz, ArH), 7.54 (dd, J = 7.6, 1.4 Hz, ArH), 7.2−7.4 (m, ArH, 2 H), 5.27 (s, NCH_2), 3.83 (s, OCH_3), 2.2−2.35 (m, C**H**CH_2CH_2), 1.2−1.4 (m, CHC**H**$_2$C**H**$_2$); MS (EI) *m/e* 337, 278, 268, 209, 195. Anal. ($C_{17}H_{15}N_5O_3$) C, H, N.

With Amines, Method F: 3-(5-Cyclopropyl-1,2,4-oxadiazol-3-yl)-4,5-dihydro-5-(pyrrolidinocarbonyl)imidazo[1,5-*a*]quinoxaline (45). A solution of carbamyl chloride **9a** (1.00 g, 2.93 mmol) and diisopropylethylamine (1.02 mL, 5.86 mmol) in 20 mL of THF was cooled in an ice bath. Pyrrolidine (0.37 mL, 4.4 mmol) was added, and the mixture was allowed to warm to room temperature and stir overnight. Basic workup (CH_2Cl_2, $NaHCO_3$, Na_2SO_4) and recrystallization from CH_2Cl_2/hexane gave 1.02 g (92%) of **45** as a white powder (mp 181.5−182.5 °C): IR (mineral oil) 3007, 1648, 1513, 1501, 1409, 1204, 760, 756 cm^{-1}; ^1H NMR (300 MHz, $CDCl_3$) δ 8.10 (s, ArH), 7.54 (d, J = 7.7 Hz, ArH), 7.1−7.3 (m, ArH, 3 H), 5.04 (s, $ArNCH_2$), 3.28 (br s, N**C**H_2CH_2, 4 H), 2.2−2.3 (m, CH), 1.75−1.9 (m, NCH_2C**H**$_2$, 4 H), 1.15−1.4 (m, CHC**H**$_2$C**H**$_2$); MS (EI) *m/e* 376, 306, 278, 238. Anal. ($C_{20}H_{20}N_6O_2$) C, H, N.

With Thiols, Method G: 3-(5-Cyclopropyl-1,2,4-oxadiazol-3-yl)-4,5-dihydro-5-[(methylthio)carbonyl]imidazo-[1,5-*a*]quinoxaline (51). Sodium thiomethoxide (158 mg, 2.25 mmol) was added to a slurry of carbamyl chloride **9a** (700 mg, 2.05 mmol) in 10 mL of THF at 0 °C. The mixture was allowed to warm to room temperature and stirred for 19 h. The concentrated material was stirred in a mixture of water and 20% ether/hexane. The resulting solids were filtered, washed with water and hexane, and dried to give 690 mg (95%) of **51** as a white solid (mp 176−177 °C): IR (mineral oil) 1660, 1497, 1422, 1357, 1206, 761 cm^{-1}; ^1H NMR (300 MHz, $CDCl_3$) δ 8.12 (s, ArH), 7.85 (d, J = 7.4 Hz, ArH), 7.58 (d, J = 7.4 Hz, ArH), 7.3−7.45 (m, ArH, 2 H), 5.34 (s, NCH_2), 2.36 (s, SCH_3), 2.25−2.4 (m, CH), 1.2−1.4 (m, CH_2CH_2); MS (EI) *m/e* 353, 306, 278, 210, 195. Anal. ($C_{17}H_{15}N_5O_2S \cdot {}^1/_4H_2O$) C, H, N, S.

Example Procedure for 12. Method H: 6-Chloro-3,3-dimethyl-1,2,3,4-tetrahydro-4-(pyrrolidinocarbonyl)-quinoxalin-2-one (12h, Nu = pyrrolidine). Phosgene (60.0 mL, 72.0 mmol, 12.5% in toluene) was added to a solution of amine **3h** (4.50 g, 21.4 mmol), THF (25.0 mL), imidazole (50 mg), and diisopropylethylamine (4.50 mL, 25.8 mmol). The solution was stirred at room temperature for 96 h. Additional phosgene (20.0 mL, 24.0 mmol), diisopropylethylamine (2.00 mL, 11.5 mmol), and CH_2Cl_2 (10 mL) were added after 24 h. Aqueous workup (ethyl acetate, $MgSO_4$) and trituration of the residue with 20:1 hexane:ether gave 5.64 g (96%) of carbamoyl chloride **11h** as a tan powder: ^1H NMR (300 MHz, $CDCl_3$) δ 9.05−9.25 (br s, NH), 7.42 (d, J = 2.1 Hz, ArH), 7.26 (dd, J = 8.5, 2.2 Hz, ArH), 6.91 (d, J = 8.5 Hz, ArH), 1.64 (s, $C(CH_3)_2$).

Pyrrolidine (2.25 mL, 27.0 mmol) was added to a solution of the crude carbamoyl chloride **11h** (5.64 g, 20.7 mmol), THF (100 mL), and diisopropylethylamine (4.70 mL, 27.0 mmol) at 0 °C. The solution was stirred for 1 h at 0 °C and for 15 h at room temperature. Aqueous workup (ethyl acetate, $MgSO_4$) and crystallization from ethyl acetate−hexane gave (two crops) 5.14 g of the desired product as white crystals (mp 192−193 °C). The filtrate was concentrated and purified by flash chromatography (1:1 ethyl acetate:hexane) to provide an additional 391 mg (5.53 g total, 84% from amine) of product: IR (mineral oil) 3203, 3077, 1691, 1661, 1503, 1416, 1390, 1380, 1354, 1301 cm^{-1}; ^1H NMR (300 MHz, $CDCl_3$) δ 8.54 (s, NH), 6.90 (dd, J = 8.3, 2.1 Hz, ArH), 6.76 (d, J = 8.3 Hz, ArH), 6.68 (d, J = 2.1 Hz, ArH), 3.58 (br s, 2 H), 3.17 (br s, 2 H), 1.2−2.0 (m, 10 H); MS (EI) *m/e* 307, 98.

Example Procedure for Acylation of 3. Method I: 4-(2-Furoyl)-1,2,3,4-tetrahydroquinoxalin-2-one (12a, Nu = 2-furan). 2-Furoyl chloride (0.49 mL, 5.0 mmol) was added to a solution of amine **3a** (710 mg, 4.79 mmol), triethylamine (0.80 mL, 5.7 mmol), and THF (20 mL) at 0 °C. The mixture was stirred for 1.5 h at 0 °C and for 2 h at room temperature. Basic workup (ethyl acetate and then $CHCl_3$, $NaHCO_3$, $MgSO_4$) and recrystallization from hot ethyl acetate gave 815 mg (70%) of the desired product as off-white needles (mp 229−230 °C): IR (mineral oil) 1684, 1648, 1504, 1474, 1391, 1373, 756 cm^{-1}; ^1H NMR (300 MHz, $CDCl_3$) 8.53 (br s, NH), 7.39 (s, ArH), 7.1−7.25 (m, ArH), 6.85−7.05 (m, ArH, 4 H), 6.45 (dd, J = 3.5, 1.7 Hz, ArH), 4.59 (s, NCH_2); MS (EI) *m/e* 242, 95.

Example Procedure for the Reaction of 12 with Isocyanide 5. Method J: 7-Chloro-3-(5-cyclopropyl-1,2,4-oxadiazol-3-yl)-4,4-dimethyl-4,5-dihydro-5-(pyrrolidinocarbonyl)imidazo[1,5-*a*]quinoxaline (74). Potassium *tert*-butoxide (2.05 mL, 2.05 mmol, 1.0 M in THF) was added to a solution of amide **12h** (Nu = pyrrolidine; 626 mg, 2.03 mmol) and THF (3.2 mL) at −25 °C. The solution was allowed to warm to 0 °C over 45 min and recooled to −40 °C. Diethyl chlorophosphate (0.30 mL, 2.1 mmol) was added, and the solution was allowed to warm to 0 °C over 1 h. After cooling to −78 °C, a solution of isocyanide **5** (333 mg, 2.23 mmol) and THF (0.5 mL) was added. Potassium *tert*-butoxide (2.05 mL, 2.05 mmol) was then added dropwise over several minutes.

The reddish solution was stirred at −78 °C for 30 min and allowed to warm slowly to room temperature. After 16 h, aqueous workup (ethyl acetate, $MgSO_4$), trituration (10:1 hexane:ether), and recrystallization of the resultant solid from hot ethyl acetate−hexane gave 620 mg (70%, three crops) of **74** as off-white needles (mp 207−208 °C): IR (mineral oil) 3118, 1653, 1588, 1518, 1416, 1187, 945 cm^{-1}; ^{1}H NMR (300 MHz, $CDCl_3$) δ 8.07 (s, ArH), 7.41 (d, J = 8.5 Hz, ArH), 7.00 (dd, J = 8.5, 2.1 Hz, ArH), 6.80 (d, J = 2.1 Hz, ArH), 3.59 (br s, 2 H), 2.8−3.4 (m, 2 H), 2.2−2.35 (m, C**H**CH_2), 1.5−2.2 (m, C(C**H**$_3$)$_2$, NCH_2C**H**$_2$C**H**$_2$), 1.15−1.45 (m, CHC**H**$_2$C**H**$_2$); MS (EI) *m*/*e* 438, 423, 98. Anal. ($C_{22}H_{23}N_6O_2Cl$) C, H, N, Cl.

GABA$_A$ Receptor Expression and Membrane Preparation. DNA manipulations and general baculovirus methods (Sf-9 cell cultivation, infection, and isolation, purification of recombinant viruses) were performed as described elsewhere.[26] The Sf-9 cells were infected at a multiplicity of infection of 3 plaque-forming units of viruses: AcNPV-α_1, -α_3, or -α_6, AcNPV-β_2, and AcNPV-γ_2. Infected cells were used for electrophysiological measurements at 48 h postinfection or for membrane preparations at 60 h postinfection. The stable cell lines expressing α_1 or α_3, α_6, β_2, and γ_2 subunits of GABA$_A$ were derived by transfection of plasmids containing cDNA and a plasmid encoding G418 resistance into human kidney cells (A293 cells) as described elsewhere.[27] After 2 weeks of selection in 1 mg/mL G418, cells positive for all three GABA$_A$ receptor mRNAs by Northern blotting were used for electrophysiology to measure GABA-induced Cl^- currents. For equilibrium binding measurements, Sf-9 cells infected with baculovirus-carrying cDNAs for α_1 or α_3, α_6, β_2, and γ_2 subunits were harvested in 2 L batches 60 h postinfection. The membranes were prepared following the procedure described previously.[26] Briefly, the membranes were prepared in normal saline after homogenization with Polytron PT 3000 homogenizer (Brinkman) for 4 min. Unbroken cells and large nuclei aggregates were removed by centrifugation at 1000*g* for 10 min. Then the membranes were recovered with the second centrifugation of the supernatant at 40000*g* for 50 min. The membranes were resuspended to a final concentration of 5 mg/mL in a solution containing 300 mM sucrose, 5 mM Tris/HCl, pH 7.5, and glycerol to a final concentration of 20% and stored at −80 °C. Equilibrium binding of [^{3}H]flunitrazepam or [^{3}H]Ro-4513 to the cloned GABA$_A$ receptors was measured in a 500 μL volume of normal saline containing 6 nM [^{3}H]-flunitrazepam or [^{3}H]Ro-4513, varying concentrations of test ligands, and 50 μg of membrane protein. The mixture was incubated for 60 min at 4 °C, filtered over a Whatman glass fiber filter, and washed four times with cold normal saline. The filter was then counted for radioactivity in the presence of a scintillation cocktail (Insta Gel).

GABA$_A$ Receptor Binding. The *in vitro* binding affinity of the imidazo[1,5-*a*]quinoxalines for GABA$_A$ was determined as previously described with minor modification.[17] Freshly prepared rat cerebellar membranes were suspended in 300 mM sucrose and 10 nM Hepes/Tris, pH 7.4. Typically, the reaction medium contained 6 mM [^{3}H]flunitrazepam, 50 μg of membrane protein, test drugs at various concentrations or vehicle in 200 μL, 118 nM NaCl, 10 mM Hepes/Tris, pH 7.4, and 1 mM $MgCl_2$. The mixtures were incubated for 60 min at 4 °C. The amount of binding was determined with rapid filtration techniques using Whatman GF/B filters.

[^{35}S]-*tert*-Butyl Bicyclophosphorothionate ([^{35}S]TBPS) Binding. Binding of [^{35}S]TBPS in the rat brain membranes was measured in the medium containing 2 nM [^{35}S]TBPS, unless specified otherwise, 50 μg of membrane proteins, 1 M NaCl, and 10 mM Tris/HCl, pH 7.4, in a total volume of 500 μL. Drugs were added in concentrated methanolic solutions, and the level of methanol did not exceed 0.2% and was maintained constant in all tubes. The mixtures were incubated for 120 min at 24 °C. The reaction mixtures were filtered over a Whatman GF/B filter under vacuum. The filters were washed three times with 4 mL of the reaction buffer without radioisotope and counted for radioactivity. Nonspecific binding was estimated in the presence of 2 μM diazepam or unlabeled TBPS and subtracted to compute specific binding.[18]

$^{36}Cl^-$ Uptake Studies. $^{36}Cl^-$ uptake in rat cerebrocortical synaptoneurosomes was measured by a rapid filtration technique using Whatman GF/B filters as described elsewhere.[18,19] A typical incubation medium contained 0.2 μCi Na^{36}Cl/mL, 118 mM NaCl, 5 mM KCl, 1.8 mM $MgSO_4$, and 20 mM Hepes/Tris, pH 7.0, with or without test drugs. Drugs were added in concentrated methanol solutions, and the level of methanol did not exceed 0.4% and was maintained constant in all tubes. The membrane suspensions were preincubated for 5 min at 30 °C. The reaction was initiated by mixing equal volumes (125 μL) of the membrane suspension (1 mg of protein) and the reaction mixture containing $^{36}Cl^-$ at 30 °C. After 5 s, the reaction was terminated by adding ice cold NaCl incubation buffer. The mixture was filtered over a Whatman GF/B filter under vacuum, and the filters were washed four times with 5 mL of ice cold NaCl incubation buffer. The radioactivity on the filters was counted in the presence of Instagel (15 mL).

Electrophysiology. The whole cell configuration of the patch clamp technique was used to record the GABA-mediated Cl^- currents in the A293 cells expressing the $\alpha_1\beta_2\gamma_2$ subtype, as described earlier.[20] Briefly, patch pipettes made of borosilicate glass tubes were fire-polished and showed a tip resistance of 0.5−2 MΩ when filled with a solution containing (mM) 140 CsCl, 11 EGTA, 4 $MgCl_2$, 2 ATP, and 10 Hepes, pH 7.3. The cell-bathing external solution contained (mM) 135 NaCl, 5 KCl, 1 $MgCl_2$, 1.8 $CaCl_2$, and 5 Hepes, pH 7.2 (normal saline). GABA at the concentration of 5 μM in the external solution with or without indicated drugs was applied through a U-tube placed within 100 μm of the cells for 10 s, unless indicated otherwise. The current was recorded with an Axopatch 1D amplifier and a CV-4 headstage (Axon Instrument Co.). A Bh-1 bath headstage was used to compensate for changes in bath potentials. The currents were recorded with a Gould Recorder 220. GABA currents were measured at the holding potential of −60 mV at room temperature (21−24 °C).

Metrazole Antagonism. Compounds were tested for their ability to antagonize metrazole-induced convulsions in rats after ip injection as described elsewhere.[21] Briefly, male CF-1 mice were injected with metrazole (85 mg/kg, sc), and convulsive seizure was elicited 15 min later with an auditory stimulation (5 dB for 10 s). Drugs tested for metrazole antagonism were injected ip 30 min before the metrazole challenge, 4 mice/dose at a 0.3 log dose interval. ED_{50}s for protection against tonic seizure were calculated by the method of Spearman-Karber (Finney, D. J. *Statistical Methods in Biological Assay*).

Ethanol Potentiation. Male CF-1 Charles River mice were injected orally with 7.5 mL/kg 50% aqueous ethanol and simultaneously received the test compound by the subcutaneous route (10 mL/kg in 0.25% aqueous methyl cellulose). Thirty minutes later, they were tested for the loss of traction response (muscle relaxation) and loss of righting reflex (anesthesia). The former test consists of determining if the mouse after suspension by the forepaws on an 18 g wire can place one of its hindlimbs on the wire within 10 s. The latter test determines whether the same animal will roll over onto its feet within 10 s of release on its back. Six mice were tested at each dose, and active compounds were retested at several doses to establish an ED_{50}.

Acute Physical Dependence.[28] Male CF-1 mice (10/group) were dosed sc twice daily with the test compound, once at 0800 and again at 1600 (with twice the 0800 dose) for 3 days. Twenty-four hours after the last dose, they received an intravenous injection of the benzodiazepine antagonist flumazenil (2.5 mg/kg in 5% aqueous *N*,*N*-dimethylacetamide). Five minutes later, the electroshock seizure threshold was estimated by the up−down method in which the stimulus current was lowered or elevated by 0.05 log interval if the preceding animal did or did not convulse, respectively. From the data thus generated, a threshold (effective current 50) was calculated. The other parameters of the transpinnal (e.g., delivered across the ears via saline-soaked ear clip electrodes) square wave stimulation were held constant (0.6 ms pulses at 100 Hz for 0.2 s). Test compounds, the precipitated withdrawal from which significantly lowered (below 95% confidence in-

terval of parallel control group treated for 3 days with saline and injected intravenously with flumazenil) the seizure threshold, were considered to have caused physical dependence.

Benzodiazepine Antagonism. Male CF-1 Charles River mice were injected ip simultaneously with 1 mg/kg triazolam and test compound starting at 100 mg/kg. A dose−response was run on a 0.5 log scale. All drugs were made up in No. 122 sterile vehicle (0.25% aqueous methyl cellulose). Fifteen minutes later, they were tested for loss of traction response (muscle relaxation) as indicated above. If the expected loss of traction in response to triazolam was not observed, the test compound was assumed to be an antagonist. Lower doses (at 0.5 log intervals) of the test compound were then evaluated to establish the antagonist dose$_{50}$ (ED$_{50}$).

Vogel's Punished Licking Assay. Following a previously reported procedure,[10a] experimentally naive, male F344 rats were deprived of drinking water for 48 h before being placed in a chamber with a drinking spout. Brief electric shock (0.5 mA, 0.1 s) was delivered through the spout during every 10th lick. The session terminated 3 min after the first shock or 15 min after the session started if no drinking occurred. A test drug was injected ip 30 min before the test session, with at least 8 animals/dose group. The median number of shocks for each dose group was compared to that of a parallel vehicle-treated group, using a one-way analysis of variance followed by the nonparametric Wilcoxon rank sum test.

Geller−Cook Conflict Test. Following a previously reported procedure,[10a] male Sprague−Dawley rats were trained to press a lever for food reinforcement (45 mg pellet). A 5 min period of VI-60" schedule alternated with a 2 min period of FR-10 punishment schedule, where each food delivery was accompanied by electrical shock (0.4 mA, 0.5 s) from the grid floor. The punishment component was always signaled by a light over the response lever. After performance stabilized, test drugs or vehicle was injected ip 30 min before the session, with at least 6 animals/dose group. A drug effect for each rat was measured by the increase of shocks compared to the immediately preceding vehicle session. Statistical significance for each dose was estimated by the Wilcoxon signed-rank test.

References

(1) (a) Squires, R., Ed. *GABA and Benzodiazepine Receptors*; CRC Press: Boca Raton, FL, 1988; Vol. I, II. (b) Haefely, W. In *Benzodiazepines*; Beaumont, G., Brandon, S., Leonard, B. E., Eds.; John Wiley and Sons: New York, 1990; pp 1−18. (c) Haefely, W. Partial Agonists of the Benzodiazepine Receptor: From Animal Data to Results in Patients. In *Chloride Channels and Their Modulation by Neurotransmitters and Drugs*; Biggio, G., Costa, E., Eds.; Raven Press: New York, 1988; pp 275−292.

(2) (a) Gardner, C. R. Functional *In Vivo* Correlates of the Benzodiazepine Agonist-Inverse Agonist Continuum. *Prog. Neurobiol.* **1988**, *31*, 425−476. (b) Braestrup, C.; Nielsen, M. In *Receptor Biochemistry and Methodology*; Olsen, R. W., Venter, J. C., Eds.; A. R. Liss, Inc.: New York, 1986; Vol. 5, p 167. (c) Bare, T. M.; Resch, J. F.; Patel, J. B. Anxiolytics and Sedative-Hypnotics. In *Annual Reports in Medicinal Chemistry*; Bailey, D. M., Ed.; Academic Press: New York, 1987; Vol. 22, pp 11−20. (d) Haefely, W.; Kyburz, E.; Gerecke, M.; Mohler, H. Recent Advances in the Molecular Pharmacology of Benzodiazepine Receptors and in the Structure-Activity Relationships of Their Agonists and Antagonists. In *Advances in Drug Research*; Testa, B., Ed.; Academic Press: New York, 1985; Vol. 14, pp 165−322. (e) Braestrup, C.; Honore, T.; Nielsen, M.; Petersen, E. N.; Jensen, L. H. Ligands for Benzodiazepine Receptors With Positive and Negative Efficacy. *Biochem. Pharmacol.* **1984**, *33*, 859−862.

(3) (a) Petersen, E. N.; Jensen, L. H.; Diejer, J.; Honore, T. New Perspectives in Benzodiazepine Receptor Pharmacology. *Pharmacopsychiatry* **1986**, *19*, 4−6. (b) Haefely, W. Psychopharmacology of Anxiety. *Eur. Neuropsychopharmacol.* **1991**, *1*, 89−95.

(4) (a) Pritchett, D. B.; Sontheimer, H.; Shivers, B. D.; Ymer, S.; Kettenmann, H.; Schonfield, P. R.; Seeburg, P. H. Importance of a Novel GABA$_A$ Receptor Subunit for Benzodiazepine Pharmacology. *Nature* **1989**, *338*, 582−585. (b) Pritchett, D. B.; Seeburg, P. H. γ-Aminobutyric Acid Type A Receptor Point Mutation Increases the Affinity of Compounds for the Benzodiazepine Site. *Proc. Natl. Acad. Sci. U.S.A.* **1991**, *88*, 1421−1425.

(5) Skolnick, P.; Wong, G. In *Imidazopyridines in Anxiety Disorders: A Novel Experimental and Therapeutic Approach*; Zivkovic, B., Langer, S., Bartholini, G., Eds.; Raven Press: New York, 1992.

(6) (a) Stephens, D. N.; Schneider, H. H.; Kehr, W.; Andrews, J. S.; Rettig, K.-J.; Turski, L.; Schmiechen, R.; Turner, J. D.; Jensen, L. H.; Petersen, E. N.; Honore, T.; Bondo Hansen, J. Abecarnil, a Metabolically Stable, Anxioselective β-Carboline Acting at Benzodiazepine Receptors. *J. Pharmacol. Exp. Ther.* **1990**, *253*, 334−343. (b) Turski, L.; Stephens, D. N.; Jensen, L. H.; Petersen, E. N.; Meldrum, B. S.; Patel, S.; Bondo Hansen, J.; Loscher, W.; Schneider, H. H.; Schmiechen, R. Anticonvulsant Action of the β-Carboline Abecarnil: Studies in Rodents and Baboon, *Papio papio*. *J. Pharmacol. Exp. Ther.* **1990**, *253*, 344−352. (c) Ballenger, J. C.; McDonald, S.; Noyes, R.; Rickels, K.; Sussman, N.; Woods, S.; Patin, J.; Singer, J. The First Double-Blind, Placebo-Controlled Trial of a Partial Benzodiazepine Agonist Abecarnil (ZK 112−119) in Generalized Anxiety Disorder. *Psychopharmacol. Bull.* **1991**, *27*, 171−179.

(7) (a) Pieri, L.; Hunkeler, W.; Jauch, R.; Merz, W. A.; Roncari, G.; Timm, U. Ro 16-6028. *Drugs Future* **1988**, *13*, 730−735. (b) Haefely, W.; Martin, J. R.; Schoch, P. Novel Anxiolytics That Act as Partial Agonists at Benzodiazepine Receptors. *TIPS* **1990**, *11*, 452−456.

(8) Morimoto, Y.; Fukuda, T.; Yakushiji, T.; Takehara, S.; Anami, K.; Yamamoto, Y.; Yasumatsu, H.; Nakao, T.; Setoguchi, M.; Tahar, T. Anxiolytic Properties of Y-23684, a Benzodiazepine Receptor Partial Agonist in Comparison with Diazepam. Proc. 17th CINP Congr., Kyoto, 1990; Abstr. P-12-2-9, p 169.

(9) George, P.; Rossey, G.; Depoortere, H.; Mompon, B.; Allen, J.; Wick, A. Imidazopyridines: Towards Novel Hypnotic and Anxiolytic Drugs. *Farmaco* **1991**, *46* (Suppl.), 277−288.

(10) (a) Tang, A. H.; Franklin, S. R.; Himes, C. S.; Ho, P. M. Behavioral Effects of U-78875, a Quinoxalinone Anxiolytic with Potent Benzodiazepine Antagonist Activity. *J. Pharmacol. Exp. Ther.* **1991**, *259*, 248−254. (b) Petke, J. D.; Im, H. K.; Im, W. B.; Blakeman, D. P.; Pregenzer, J. F.; Jacobsen, E. J.; Hamilton, B. J.; Carter, D. B. Characterization of Functional Interactions of Imidazoquinoxaline Derivatives with Benzodiazepine-γ-Aminobutyric Acid$_A$ Receptors. *Mol. Pharmacol.* **1992**, *42*, 294−301.

(11) DN-2327. *Drugs Future* **1993**, *18* (5), 414−417.

(12) TenBrink, R. E.; Im, W. B.; Sethy, V. H.; Tang, A. H.; Carter, D. B. Antagonist, Partial Agonist, and Full Agonist Imidazo-[1,5-*a*]quinoxaline Amides and Carbamates Acting through the GABA$_A$/Benzodiazepine Receptor. *J. Med. Chem.* **1994**, *37*, 758−768.

(13) Im, W. B.; Im, H. K.; Pregenzer, J. F.; Hamilton, B. J.; Carter, D. B.; Jacobsen, E. J.; TenBrink, R. E.; VonVoigtlander, P. F. Differential Affinity of Dihydroimidazoquinoxalines and Diimidazoquinazolines to the $\alpha_1\beta_2\gamma_2$ and $\alpha_6\beta_2\gamma_2$ Subtypes of Cloned GABA$_A$ Receptors. *Br. J. Pharmacol.* **1993**, *110*, 677−680.

(14) Watjen, F.; Baker, R.; Engelstoff, M.; Herbert, R.; MacLeod, A.; Knight, A.; Merchant, K.; Moseley, J.; Saunders, J.; Swain, C. J.; Wong, E.; Springer, J. P. Novel Benzodiazepine Receptor Partial Agonists: Oxadiazolylimidazobenzodiazepines. *J. Med. Chem.* **1989**, *32*, 2282−2291.

(15) Lumma, W. C.; Hartman, R. D.; Saari, W. S.; Englehardt, E. L. Piperazinylquinoxalines With Central Serotoninmimetic Activity. *J. Med. Chem.* **1981**, *24*, 93−101.

(16) Djerassi, C.; Engle, R. R.; Bowers, A. The Direct Conversion of Steroidal Δ^5-3β-Alcohols to Δ^5- and Δ^4-3-Ketones. *J. Org. Chem.* **1956**, *21*, 1547−1549.

(17) Sethy, V. H.; Harris, D. W. Determination of Biological Activity of Alprazolam, Triazolam and Their Metabolites. *J. Pharm. Pharmacol.* **1982**, *34*, 115−116.

(18) Im, W. B.; Blakeman, D. P. Correlation Between γ-Aminobutyric Acid$_A$ Receptor Ligand-Induced Changes in t-Butylbicyclophosphoro[^{35}S]thionate Binding and $^{36}Cl^-$ Uptake in Rat Cerebrocortical Membranes. *Mol. Pharmacol.* **1991**, *39*, 394−398.

(19) Schwartz, R. D.; Suzdak, P. D.; Paul, S. M. γ-Aminobutyric Acid (GABA)- and Barbiturate-Mediated $^{36}Cl^-$ Uptake in Rat Brain Synaptoneurosomes: Evidence for Rapid Desensitization of the GABA Receptor-Coupled Chloride Ion Channel. *Mol. Pharmacol.* **1986**, *30*, 419−426.

(20) Im, H. K.; Im, W. B.; Hamilton, B. J.; Carter, D. B.; VonVoigtlander, P. F. Potentiation of GABA-induced Chloride Currents by Various Benzodiazepine Site Agonists with $\alpha_1\gamma_2$, $\beta_2\gamma_2$ and $\alpha_1\beta_2\gamma_2$ Subtypes of Cloned GABA$_A$ Receptors. *Mol. Pharmacol.* **1993**, *44*, 866−870.

(21) Rudzik, A. D.; Hester, J. B.; Tang, A. H.; Straw, R. N.; Friis, W. Triazolobenzodiazepines, A New Class of Central Nervous System-Depressant Compounds. In *The Benzodiazepines*; Garatini, S., Mussini, E., Randall, L. O., Eds.; Raven Press: New York, 1973; pp 285−297.

(22) These standards had ED$_{50}$s in the range of 0.17−4.5 mg/kg.

(23) (a) Pritchett, D. B.; Seeburg, P. H. γ-Aminobutyric Acid$_A$ Receptor α_5-Subunit Creates Novel Type II Benzodiazepine Receptor Pharmacology. *J. Neurochem.* **1990**, *54*, 1802−1804. (b) Pritchett, D. B.; Luddens, H.; Seeburg, P. H. Type I and Type II GABA$_A$-Benzodiazepine Receptors Produced in Transfected Cells. *Science* **1989**, *245*, 1389−1392.

(24) Luddens, H.; Pritchett, D. B.; Kohler, M.; Killisch, I.; Keinanen, K.; Monyer, H.; Sprengel, R.; Seeburg, P. H. Cerebellar $GABA_A$ Receptor Selective for a Behavioral Alcohol Antagonist. *Nature* **1990**, *346*, 648−651.
(25) Puia, G.; Vicini, S.; Seeburg, P. H.; Costa, E. Influence of Recombinant γ-Aminobutyric $Acid_A$ Receptor Subunit Composition on the Action of Allosteric Modulators of γ-Aminobutyric $Acid_A$-Gated Cl^- Currents. *Mol. Pharmacol.* **1991**, *39*, 691−696.
(26) Carter, D. B.; Thomsen, D. R.; Im, W. B.; Lennon, D. J.; Ngo, D. M.; Gale, W.; Im, H. K.; Seeburg, P. H.; Smith, M. W. Functional Expression of $GABA_A$ Chloride Channels and Benzodiazepine Binding Sites in Baculovirus Infected Insect Cells. *Bio/Technology* **1992**, *10*, 679−681.
(27) Hamilton, B. J.; Lennon, D. J.; Im, H. K.; Im, W. B.; Seeburg, P. H.; Carter, D. B. Stable Expression of Cloned Rat $GABA_A$ Receptor Subunits in a Human Kidney Cell Line. *Neurosci. Lett.* **1993**, *153*, 206−209.
(28) VonVoigtlander, P. F.; Lewis, R. A. A Rapid Screening Method for the Assessment of Benzodiazepine Receptor-Related Physical Dependence in Mice. *J. Pharmacol. Methods* **1991**, *26*, 1−5.
(29) Mohamadi, F.; Richards, N. G. J.; Guida, W. C.; Liskamp, R.; Lipton, M.; Caufield, C.; Chang, G.; Hendrickson, T.; Still, W. C. MacroModel-An Integrated Software System for Modeling Organic and Bioorganic Molecules Using Molecular Mechanics. *J. Comput. Chem.* **1990**, *11*, 440−467.
(30) Weiner, S. J.; Kollman, P. A.; Nguyen, D. T.; Case, D. A. An All Atom Force Field for Simulations of Proteins and Nucleic Acids. *J. Comput. Chem.* **1986**, *7*, 230−252.
(31) Allinger, N. L. Conformational Analysis. 130. MM2. A Hydrocarbon Force Field Utilizing V_1 and V_2 Torsional Terms. *J. Am. Chem. Soc.* **1977**, *99*, 8127−8134.
(32) Chang, G.; Guida, W. C.; Still, W. C. An Internal Coordinate Monte Carlo Method for Searching Conformational Space. *J. Am. Chem. Soc.* **1989**, *111*, 4379−4386.
(33) Mickelson, J. W.; Jacobsen, E. J.; Im, H. K.; Im, W. B.; Schreur, P. K. D.; Sethy, V. H.; Tang, A. H.; VonVoigtlander, P. F.; McGee, J. E.; Petke, J. D. Unpublished observations.
(34) Villar, H. O.; Davies, M. F.; Loew, G. H.; Maguire, P. A. Molecular Models for Recognition and Activation at the Benzodiazepine Receptor: A Review. *Life Sci.* **1991**, *48*, 593−602.
(35) Tebib, S.; Bourguignon, J.-J.; Wermuth, C.-G. The Active Analog Approach Applied to the Pharmacophore Identification of Benzodiazepine Receptor Ligands. *J. Comput.-Aided Mol. Des.* **1987**, *1*, 153−170.
(36) Gardner, C. R. A Review of Recently-Developed Ligands for Neuronal Benzodiazepine Receptors and Their Pharmacological Activities. *Prog. Neuro.-Psychopharmacol. Biol. Psychiatry* **1992**, *16*, 755−781.
(37) Fryer, R. I. Ligand Interactions at the Benzodiazepine Receptor. In *Comprehensive Medicinal Chemistry Volume 3*; Hansch, C., Sammes, P. G., Taylor, J. B., Eds.; Pergamon Press: New York, 1990.
(38) Maxim, N.; Zugravescu, I.; Fulga, I. Sur L'acide α-Pyrrole-Carbonique et Quelques Amides Derivees. (α-Pyrrole Carboxylic Acid and Some Amide Derivatives.) *Bull. Soc. Chim.* **1938**, *5*, 44−48.

JM940765F